

Nonlinear Vibration
Prof. Santosha Kumar Dwivedy
Department of Mechanical Engineering
Indian Institute of Technology, Guwahati

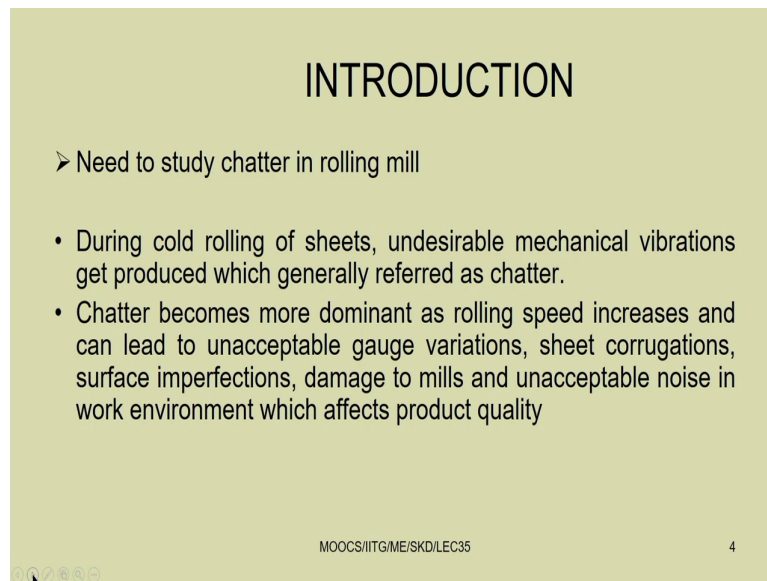
Lecture - 35

Chatter in rolling mills and dynamic analysis of artificial pneumatic muscle

Welcome to today class of Nonlinear Vibration. So, in this module we are discussing regarding several applications of non-linear vibration. So, initial classes we have studied regarding the application as a energy harvester, then we have studied the passive and active vibration observer.

So, last class we have studied regarding the application of this non-linear vibration in case of the toning problem, and today we will consider two more applications. So, for example, so in case of the cold rolling mill and then artificial muscle. So, let us see what is the chatter in case of the cold rolling mill. So, we will study the chatter in rolling mills.

(Refer Slide Time: 01:16)



INTRODUCTION

- Need to study chatter in rolling mill
- During cold rolling of sheets, undesirable mechanical vibrations get produced which generally referred as chatter.
- Chatter becomes more dominant as rolling speed increases and can lead to unacceptable gauge variations, sheet corrugations, surface imperfections, damage to mills and unacceptable noise in work environment which affects product quality

MOOCS/IITG/ME/SKD/LEC35

4

So, need to study this chatter in rolling mill you should know. So, during cold rolling of sheets, undesirable mechanical vibrations get produced we generally referred as chatter. So, chatter becomes more dominant as rolling speed increases and can lead to unacceptable gauge variations, sheet corrugations, then surface imperfections, damage to mill and unacceptable noise in work environment which affects the product quality.

So, to improve the product quality you must see that what are the parameters affecting this chatter in the rolling mill and we have to avoid this chatter. And how to avoid this chatter is also this concerned, so which we can study through these dynamics.

(Refer Slide Time: 02:08)

- Different chatter regimes in cold rolling mill
- There are three types of chatter occur in rolling mill characterized by the frequency range or musical octave of natural frequency associated with the dynamic mechanism involved
 1. torsional chatter (5-15 Hz)
 2. Third octave chatter (120-240 Hz) ✓
 3. Fifth octave chatter (550-650 Hz)

Due to gauge variations, third and fifth octave believed to be responsible for most damage to the product.

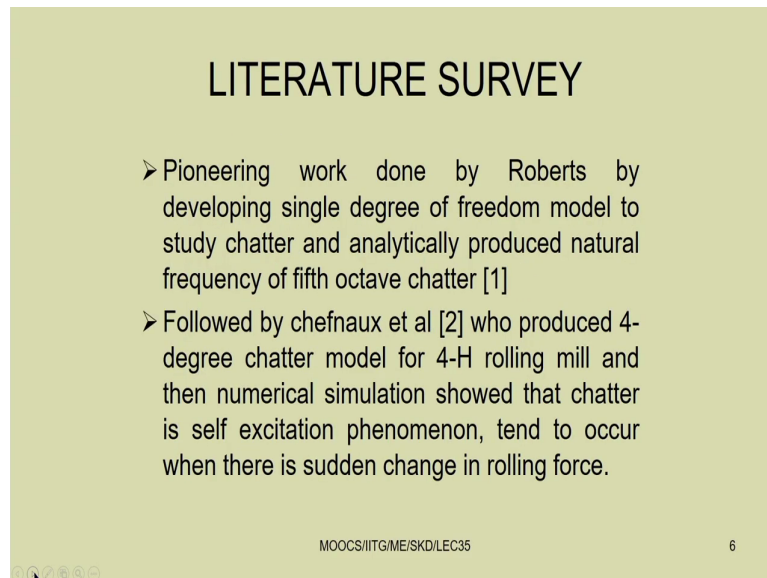
So, there are different type of chatter regimes in the cold rolling mill. So, there are three different types of chatter occur in rolling mill characterized by their frequency range or musical octave of natural frequency associated with the dynamic mechanism involved.

So, one is the torsional chatter. We generally occur from this 5 to 15 Hertz frequency. Then third octave chatter; so this is 120 to 240 Hertz frequency. Then fifth octave chatter which we can see from 550 to 650 Hertz frequency. So, generally these three types of chatter occur in this rolling mill.

So, due to gauge vibrations, third and fifth octave believe to be responsible for most damage to the products. So, we have to avoid these third and fifth octave by operating the system

away from this frequency or we have to develop some means, so that we can avoid this chatter in this field.

(Refer Slide Time: 03:16)



LITERATURE SURVEY

- Pioneering work done by Roberts by developing single degree of freedom model to study chatter and analytically produced natural frequency of fifth octave chatter [1]
- Followed by chefniaux et al [2] who produced 4-degree chatter model for 4-H rolling mill and then numerical simulation showed that chatter is self excitation phenomenon, tend to occur when there is sudden change in rolling force.

MOOCS/IITG/ME/SKD/LEC35

6

So, there are several pioneer works in this field, I will show you the literature. So, particularly this by Roberts, so who has considered the fifth octave chatter. Then by a Chefnaux et al. So, they have considered the 4 degree of freedom chatter model of a 4 high rolling mill. So, there are several rolling mills available.

So, the simplest kind of rolling mill considered in dynamics is the 4 high rolling mill. And so they have considered self-excitation, they have shown that chatter is a self excitation phenomena, tends to occur when there is sudden change in the rolling force. So, they have shown that there is due to the sudden change in the rolling force, so chatter occur in the system. So, this is self-excited vibration.

(Refer Slide Time: 04:08)

continued

- Johnson and Qi [1] developed 2-D and 4-Degree of freedom model to examine chatter phenomenon.
- Two degree model consist of squeezing mode and motion of mass centre to represent the frequency of fifth octave chatter, slightly higher because of sheet deformation force and also unsteady inter stand tension can induce instability if sufficient damping is not available
- Non-linearity and its effects also explored

MOOCS/IITG/ME/SKD/LEC35

7

Similarly, this Johnson and Qi developed 2D and 4 degrees of freedom model to examine the chatter phenomenon. Two degrees of freedom model consist of a squeezing model, squeezing mode and motion of the mass centre to represent the frequency of fifth octave chatter.

So, slightly higher because of sheet deformation force and also unsteady inter stand tension can introduce induce instability if sufficient damping is not available. So, non-linearity and its effects are also explored in this work by Johnson and Qi.

(Refer Slide Time: 04:50)

continued

- Yun et al [3] done review of different models proposed on rolling chatter in the literature so as to get better understanding of chatter.
- Correlation between different rolling parameters been proposed [4-6]. In dynamic rolling model they estimated variations in exit gage ,strip speed, tension at entry and exit ,rolling force and rolling torque in response to the variation in roll separation as well as rate of change of roll spacing [4]. Results validated using experiments and sources of chatter also recognized [5]

MOOCS/IITG/ME/SKD/LEC35

8

Similarly, Yun et al. So, they did a series of work. So, they did the review of different modes model or models proposed on rolling chatter in the literature. So, as to get better understanding of the chatter. Correlation between different rolling parameters been proposed in 4 to 6 by the same author Yun et al.

So, in dynamic rolling model they estimated variations in the exit gage, strip speed, tension at the entry and exit, rolling force and rolling torque in response to the variation in rolling separation as well as the rate of change of roll spacing. So, results validated using experiments and sources of chatter also recognized in this work.

(Refer Slide Time: 05:36)

continued

- With a chatter model they try to understand the conditions which leads to the dynamic instability and they proposed that negative damping, mode coupling and regeneration are the basic mechanisms which leads to chatter in rolling.
- There they coupled dynamic rolling model with unimodal chatter model and simulated the results to show roll force, roll gap, back tension variations leads or lags in phase to produce negative damping. In mode coupling, they took roll vibrations in more than one directions and attempted to show this as one of the causes of chatter [6].

MOOCS/IITG/ME/SKD/LEC35

9

So, with a chatter model they try to understand the conditions which leads to the dynamic instability and they proposed that negative damping, mode coupling and regeneration are the basic mechanism which lead to chatter in rolling. So, they have shown that negative damping. So, already we know how to analyze a system with negative damping, then mode coupling and this regeneration they thought are the basics of the chatter produced in the rolling mill.

So, there they coupled dynamic rolling model with unimodal chatter model and simulated the results to show roll force, roll gap, back tension variation leads to leads or lags in phase to produce negative damping. In mode coupling they took roll vibration in more than one direction and attempted to show this as one of the cause of chatter.

(Refer Slide Time: 06:39)

- A dynamic rolling model considering homogenous material also presented and here roll movement in both directions has been considered. Experimental results found in agreement with simulation results using established linearised form [7]. Ehmaan et al continued their work and produced another dynamic model considering non-homogenous material.[8]

So, then there are some other work also, pioneer work by this Ehmaan et al. So, they continued their work and the dynamic rolling model considering homogenous material also presented and here roll movement in both directions has been considered.

Experimental results found in agreement with the simulation results, using established linearization form. Ehmaan et al continued their work and produced another dynamic model considering non homogenous material also. So, this Ehmaan, so they have considered both homogenous and non homogenous material.

(Refer Slide Time: 07:18)

continued

- Friction condition in the roll bite is the source of inter stand tensions and hence the rolling mill instability. Yukio Kumara et al [9] has more to deal with friction condition in roll bite. They attempted to relate rolling conditions with vibration phenomenon through numerical simulations to put forward a theoretical rolling and chatter model of five stand continuous rolling mill and shown the influence of rolling speed and friction coefficient on vibration in rolling mill. He deduced optimal range of friction coefficients in which vibration is damped and mill is stable against the disturbance. He also proposed stability index which can give insight in to the stability of rolling mill.

So, these are very good work you can study in case of the rolling. So, there are several other work also available for example, this Yukio Kumara et al work is there and some other work by this Meehan and Rogers.

(Refer Slide Time: 07:32)

continued

- Meehan [10] developed a comprehensive stability criterion for the third octave rolling chatter and suggested a critical rolling speed below which chatter will not occur. He revealed factors which will reduce critical speed as low stand damping, low roll stand natural frequency, low slip sensitivity to tension stress, high roll force sensitivity to tension stress and geometrically thinner strips.

Fareley, Rogers [11] et al described typical resonant modes of mill stand that can become excited during third octave chatter. The interaction between third octave vibration mode and the entry strip tension have been discussed demonstrating how vibration becomes self exciting and unstable.

(Refer Slide Time: 07:40)

- Lin et al [12] presented a non-linear dynamic model of rolling chatter and initiation of fifth octave chatter. He coupled work roll sub model with roll bite sub model to produce simulation results. It concluded that even though governing dynamics is highly non-linear, rolling chatter instability is none other than mode excitation or beating and thus linear .

So, several other works are available which you can see in this, Lin et al also. So, he has his work on this instability in case of rolling mill.

(Refer Slide Time: 07:50)

Mathematical Model

- Mathematical model has been created in a view to study characteristics of fifth octave chatter.
- It consist of two parts namely 'work roll sub-model' and 'roll bite sub-model'.

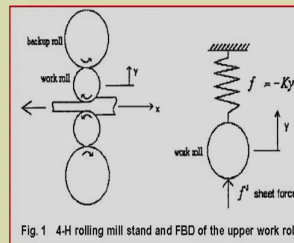
MOOCS/IITG/ME/SKD/LEC35 14

So, also you can see some of our work related to rolling mill particularly by Sajan Kapil and Eberhard. So, let us see this mathematical modeling, this work is by Shailesh (Refer Time: 08:03) who was the M. Tech student was my M. Tech student who did the did this work. So, the mathematical model has been created in a view to study the characteristic of fifth octave chatter in this case.

It consists of two parts namely work roll sub model. So, the total analysis is divided into two parts. So, one is this work roll sub model and the second one is the roll bite sub model. So, combining these two model, the rolling mill model has been developed and it is then simulated to find the response in case of this milling in case of this rolling operation.

(Refer Slide Time: 08:45)

Work Roll Sub-Model



MOOCs/IITG/ME/SKD/LEC35

15

So, this is the this is a 4 high rolling mill. So, 4 rolls you can find 4 rolls. So, here 4 rolls. So, the upper one are known as the backup roll. So, this is the backup roll and this side also with the backup roll. Then we have a work roll, so these two are the work roll which press the. So, this in got to make it in sheet form.

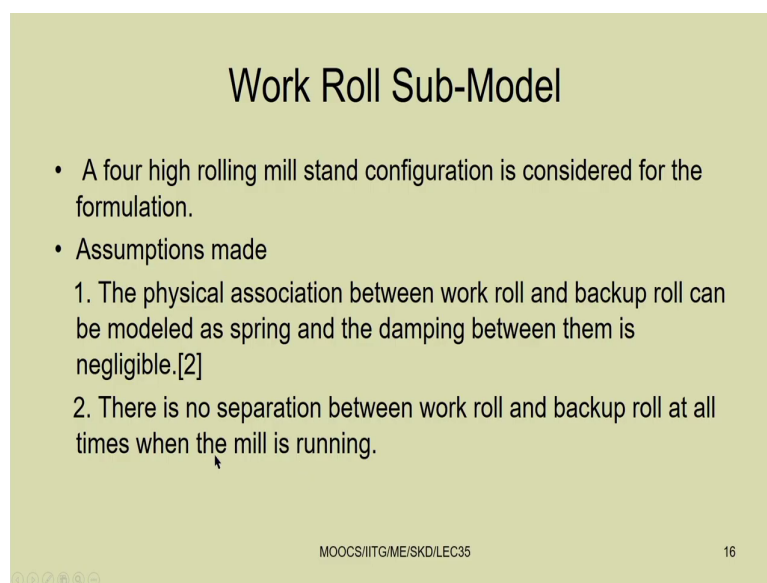
So, then, so you just see they are rotating in opposite direction and while this is rotating in clockwise direction the other one is rotating in anticlockwise direction. So, due to us both of them are rotating in opposite direction. So, the strip enters here and it get pressed and you can get a sheet.

So, this model can be represented. So, this work roll model can be represented. So, this is the sheet, the sheet will provide a force sheet force f_s . So, it will press this work roll or in turn

this work roll place the sheet. And the force between this backup roll and work roll can be modeled as a spring.

So, you can model this as a linear spring or non-linear spring. So, here it is model f equal to minus $K y$. So, y is the displacement of the work roll, so then, so this force is written as f equal to minus $K y$. So, this way you can write down this work roll sub model.

(Refer Slide Time: 10:25)



Work Roll Sub-Model

- A four high rolling mill stand configuration is considered for the formulation.
- Assumptions made
 1. The physical association between work roll and backup roll can be modeled as spring and the damping between them is negligible.[2]
 2. There is no separation between work roll and backup roll at all times when the mill is running.

MOOCs/IITG/ME/SKD/LEC35

16

So, in work roll sub model a four high rolling mill stand configuration is considered for the formulation. The assumption is that the physical association between the work roll and the backup roll can be modeled as spring and the damping between them is negligible.

So, as there is point contact, so this damping is considered to be negligible. So, there is no separation between the work roll and the backup roll at all times when the mill is running, so they are in contact. So, there is no separation between them. So, that is also the assumption.

(Refer Slide Time: 11:08)

Considering only vertical motion of work roll only,
the equation of motion along y-direction for the upper work roll becomes

$$M \frac{d^2 y}{dt^2} + Ky = f^s$$

Then, definition of spring stiffness can be given as,

$$K = \frac{df}{dy}$$

Now, displacement of work roll due to compressive load, f ,
per unit length can be given by [1]

$$y = \frac{2f(1-\mu^2)}{\pi E} \left(\frac{2}{3} + \ln \left(\frac{0.78125E(D_w + D_b)}{f(1-\mu^2)} \right) \right)$$

MOOCS/IITG/ME/SKD/LEC35 17

So, now, you have seen the we can write the equation of motion of this upper work roll like this $M \frac{d^2 y}{dt^2} + Ky = f^s$. You have seen the free body diagram. Here from the free body diagram, so you can write the equation of motion. So, this is M work roll mass is M .

So, as the motion is Y , so the inertia force is $M \ddot{Y}$. So, then this $f = K y$ equal to Ky the spring force or the force exerted by the backup and the roll and the sheet force. So, taking

all these three forces. So, the equation can be written as $M \frac{d^2 y}{dt^2} + Ky = f$.

So, the spring stiffness actually can be obtained, so by knowing the force acting between the work roll and the backup rolls. So, this force can be determined experimentally and this K can be written by $\frac{df}{dy}$. So, one can plot this f versus y , and from the slope $\frac{df}{dy}$ one can find the spring stiffness.

Now the displacement of the work roll due to compressive load f per unit length can be given by. So, from this work. So, initially we have seen. So, y can be written as $\frac{2f}{\pi E} \ln \left(\frac{D_w + D_b}{D_w - D_b} \right)$. So, $0.78125 \frac{E D_w D_b}{f} \ln \left(\frac{D_w + D_b}{D_w - D_b} \right)$.

(Refer Slide Time: 12:54)

Assuming work rolls and back rolls are of same material,

$$K = \frac{\pi E}{2(1-\mu^2) \left(\frac{-1}{3} + \ln \left(\frac{0.78125 E (D_w + D_b)}{f (1-\mu^2)} \right) \right)}$$

here the stiffness K is non linear function of sheet force

The exerted sheet force and work roll displacements can be decomposed in to steady and dynamic parts as

$$f^s = f_s^s + f_d^s \quad y_i = y_s + y_d$$

The work roll sub model can be represented as

$$M \frac{d^2 y_d}{dt^2} + K y_d = f_d^s$$

The roll gap h_c related to dynamic displacement component y_d as,

$$h_c = h_0 + 2y_d \quad h_0 = h(t=0) \quad \dot{h}_c = 2\dot{y}_d$$

MOOCS/IITG/ME/SKD/LEC35

18

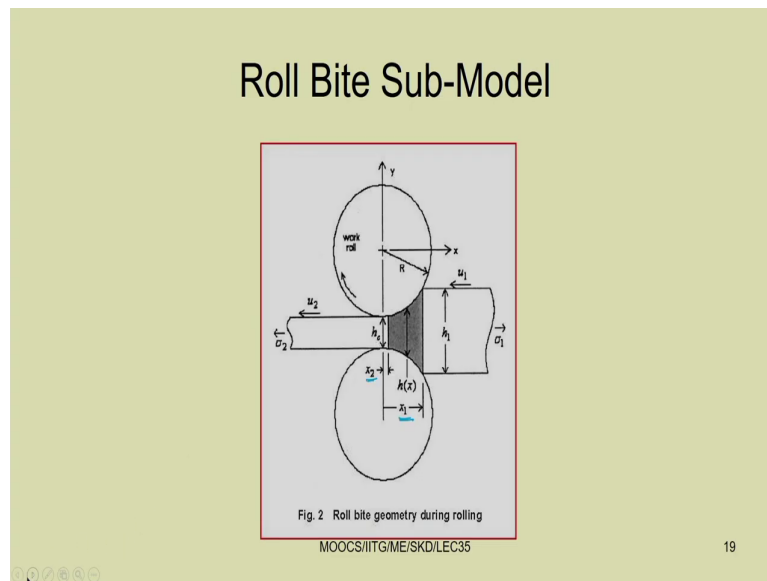
So, you can take that relation from there and then it can be K can be assuming so differentiating that thing. So, that is K . So, differentiating the thing, so the expression can be written in this form. Here the stiffness K is non-linear function of sheet. The exerted sheet force and the work roll displacement can be decomposed into steady and dynamic part so one can it can be.

So, this force can be divided into two part; one is the steady state part and the or the constant part and the dynamic part. Similarly, y can be written as the y steady part and the dynamic part. Dynamic part means which is varying with time and steady is a constant part.

The work roll sub model can be represented by $M \frac{d^2 y}{dt^2}$. So, as the differentiation of the steady part will leads to 0. So, we can have the dynamic part only we can write for the dynamic motion. So, $M \frac{d^2 y}{dt^2} = M \frac{d^2 y_d}{dt^2}$. So, this is the dynamic part of the displacement plus $K y_d$ equal to f_d .

So, the roll gap h_c can be written as $h_{c0} + 2y_d$. So, as we are considering two work rolls, so that is why. So, this roll gap can be written as $h_c = h_{c0}$, this is the initial gap plus $2y_d$. So, this h_{c0} ; that is h_c at t equal to 0 and h_c equal to. So, what? Initially then this h_c will be equal to $2y_d$.

(Refer Slide Time: 14:39)



So, then we can see the roll bite model. So, in the roll bite models we can consider this trace acting on the sheet. So, the side for example, let us take this is σ_2 this is σ_1 . So, due to, so that is a tension. So, in this thing and u_1 is the velocity in this side. It is inlet side and u_2 is the velocity of the strip in the outlet side.

So, this is initial gap roll gap, so h can be written this thing. So, this is the h and this is the entry. So, at this entry, so at a distance x_1 and it is let us consider the radius of the roll equal to R . So, we have taken this direction as the x direction as this as the y direction.

(Refer Slide Time: 15:38)

Roll Bite Sub-Model

- Figure (2) shows the roll bite of a metal sheet being rolled between two work rolls, which follow from the work of Hu and Ehmaan [7, 8].
- metal sheet is homogenous and ideally elastic plastic to which the Tresca's maximum shear stress failure criterion is applicable.

MOOCS/IITG/ME/SKD/LEC35

20

So, we can write. So, figure 2 shows the roll bite of a metal sheet being rolled between two work roll which follow from the work of Hu and Ehmaan et al, Ehmaan. So, metal sheet is homogenous and ideally elastic plastic which the Tresca's maximum shear stress failure criterion is applicable.

(Refer Slide Time: 16:00)

Using the parabolic approximation of roll bite [7],
the strip thickness within the roll bite at location x is,

$$h(x) = h_c + \frac{x^2}{R}$$

Applying the principle of conservation of material flow volume, the material flow through a vertical cross section at a distance x can be written as [7]

$$u(x)h(x) = u_1 h_1 - (x_1 - x) \dot{h}_c$$

Tresca's maximum shear stress criterion for the plane stress condition is defined as

$$\tau_y^2 = \frac{1}{4}(\sigma_{xx} - \sigma_{yy})^2 + \tau_{xy}^2$$

And a friction factor definition as

$$\tau_s = \pm m \tau_y$$

The simplified criterion for homogenous deformation as

$$(\sigma_{xx} - \sigma_{yy}) = 2\tau_y$$

MOOCs/IITG/ME/SKD/LEC35 21

So, using that criteria, so the mathematical module has been developed. So, using parabolic approximation of the roll bite. So, the strip thickness within the roll bite as a location x can be written as $h(x)$ will be equal to h_c plus x^2 by R . So, applying this principle of conservation of material flow volume, the material flow through a vertical cross section at a distance x can be written as $u(x)h(x) = u_1 h_1 - (x_1 - x) \dot{h}_c$.

Tresca's maximum shear stress criterion for the plane stress condition can be defined. So, τ_y^2 equal to $\frac{1}{4}(\sigma_{xx} - \sigma_{yy})^2 + \tau_{xy}^2$. So, and a friction factor definition can be taken τ_s equal to $\pm m \tau_y$. The simplified criterion for homogenous deformation can be taken $\sigma_{xx} - \sigma_{yy}$ will be equal to $2\tau_y$.

(Refer Slide Time: 17:07)

Now, the distance x_1 , measuring from strip to centerline of rolls is

$$x_1 = \sqrt{(h_1 - h_2)R}$$

And the strip exit position

$$x_2 = \frac{R h_c h_c}{2(u_1 h_1 - x_1 h_c)}$$

The roll bite gap at exit position is thus

$$h_2 = h_c + \frac{x_2^2}{R}$$

The static equilibrium position for vertical slide in

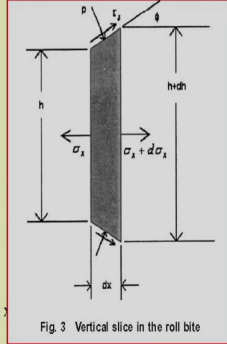


Fig. 3 Vertical slice in the roll bite

$$(\sigma_x + d\sigma_x)(h + dh) \pm 2\tau_s \sqrt{dx^2 + \frac{dh^2}{4}} \cos \phi + 2p \sqrt{dx^2 + \frac{dh^2}{4}} \sin \phi = \sigma_x h$$

Where,

$$\cos \phi = \frac{dx}{\sqrt{dx^2 + \frac{dh^2}{4}}} \quad \sin \phi = \frac{dh/2}{\sqrt{dx^2 + \frac{dh^2}{4}}}$$

MOOCS/IITG/ME/SKD/Lecture 85

22

So, taking all these approximation. So, now, the distance x_1 measuring from the strip. So, distance x_1 measuring from the strip to centerline of the roll is x_1 equal to h_1 minus h_2 . So, this is h . So, this is h plus Δh taking h plus Δh . So, we can find this x_1 equal to h_1 minus h_2 into R root over, and the strip exit position. So, this is the entry position. So, entry position. So, from the previous figure also.

So, this is, so from the centerline of the centerline of the roll. So, you can find this distance as the entry and this is the exit. So, it will exit at here, this is entry. So, it is this is a small strip is shown; entry exit you can see from the previous figure also. So, from this figure, so you can see so from the centerline so this is x_2 that is exit.

So, it exit at here. So, it is parabolic. So, you have considered a parabolic strip. So, here it is entry, clearly you can see this part is x_1 . So, this is x_1 entry and this is exit. So, at this point we are assuming to be exit; that means, after this thing the thickness becomes uniform.

So, here this to this the deformation takes place, so it is pressing two half this deformation here. So, taking a small strip so, we can write down. So, this is σ_x , this side it is σ_x , this side it is $\sigma_x + d\sigma_x$. So, this height is $h + dh$, here the height is h , so at a distance dx . So, after x we are taking a small strip of distance dx . So, the exit can be written as $R h_c$ into h_c by 2 into $u_1 h_1$ minus x_1 into h_c .

So, this so the roll bite gap at exit position is thus h_2 equal to h_c plus this is the initial gap h_c plus x_2^2 square by R . The static equilibrium position for the vertical side so can be obtained from this expression. So, doing this force balance. So, you can do this thing. So, $\sigma_x + d\sigma_x$. So, this is $\sigma_x + d\sigma_x$ then this, so multiplied by this area so thickness will be same.

So, this so or width will be same, so taking that thing $\sigma_x + d\sigma_x$ into $h + dh$ plus minus $2 \tau_s$ root over dx^2 square plus dh^2 square by 4 $\cos \phi$ plus $2p$ root over dx^2 square plus dh^2 square by 4 $\sin \phi$ equal to σ_x into h . So, where $\cos \phi$ equal to. So, you can see. So, this is the angle ϕ .

So, with the horizontal, so this is the this line is the c . So, this angle is ϕ , do this $\cos \phi$ equal to dx by root over dx^2 square plus dh^2 square by 4 and $\sin \phi$ equal to dh by 2 into dx^2 square plus dh^2 square by 4.

(Refer Slide Time: 20:28)

Can be further simplified as

$$\frac{dh}{dx}(\sigma_x + p) + h \frac{d\sigma_x}{dx} \pm 2\tau_y = 0$$

Where, the sign of friction term determined by position, of x. At the right hand side of neutral position, x_n , the friction is positive, and on the side it is negative. The horizontal stress distribution at arbitrary position x can be

$$\sigma_x = \sigma_1 + \int_{x_1}^x \frac{2\tau_y}{h(x)} \left(\mp m - \frac{2x}{R} \right) dx$$

$$\sigma_x = \sigma_1 + 2\tau_y (m_1 + m_2) \left[\frac{R}{h_c} \tan^{-1} \left(\frac{x_n}{\sqrt{R h_c}} \right) - 2\tau_y \sqrt{\frac{R}{h_c}} \left[m_1 \tan^{-1} \left(\frac{x_1}{\sqrt{R h_c}} \right) + m_2 \tan^{-1} \left(\frac{x_2}{\sqrt{R h_c}} \right) \right] - 2\tau_y \ln \left(\frac{h(x)}{h_1} \right) \right]$$

considering σ_2 at location x_2 , then

$$x_n = \sqrt{R h_c} \tan \left[\frac{m_1}{m_1 + m_2} \tan^{-1} \left(\frac{x_1}{\sqrt{R h_c}} \right) + \frac{1}{2\tau_y (m_1 + m_2)} \left(\frac{h}{R} (\sigma_2 - \sigma_1 + 2\tau_y \ln \frac{h_2}{h_1}) \right) \right]$$

MOOCJITGATEWAY

So, taking this way so it can be further simplified this dh by dx into $\sigma_x + p + h \frac{d\sigma_x}{dx} \pm 2\tau_y = 0$, so where the sign of friction term determined by the position of x . All the right-hand side of the neutral position x_n , the friction is positive, and on the side on the side is negative.

The horizontal stress distribution at arbitrary position x can be written as σ_x equal to $\sigma_1 + \int_{x_1}^x \frac{2\tau_y}{h(x)} \left(\mp m - \frac{2x}{R} \right) dx$. So, σ_x . So, you can write in this form. Then considering σ_2 location x_2 then x_n can be found here that is x_n is the neutral position. So, neutral where it is changing, the sign is changing from negative to positive, so x_n can be found.

(Refer Slide Time: 21:30)

The roll bite gap at neutral position is

$$h_n = h_c + \frac{x_n^2}{R}$$

Normal pressure p is given by

$$p(x) = 2\tau_y - (\sigma_1 + \int_{x_1}^x \frac{2\tau_y}{h(x)} (\mp m - \frac{2x}{R}) dx)$$

Then the resultant sheet deformation force can be calculated as

$$f^s = \int_{x_2}^{x_1} p(x) dx + \int_{x_2}^{x_1} \mp \tau_s \tan \phi dx$$

Expanding above equation yields vertical sheet force

$$f^s = (2\tau_y + \sigma_1)(x_2 - x_1) + \frac{\tau_y}{R} [m_2(x_2^2 - x_n^2) + m_1(x_1^2 - x_n^2)] +$$

$$\tau_y R m_2 \ln\left(\frac{h_2}{h_n}\right) + \tau_y R m_1 \ln\left(\frac{h_1}{h_n}\right) + 2\tau_y x_2 \ln\left(\frac{h_2}{h_2}\right) + 2\tau_y (m_1 + m_2) x_2 \sqrt{\frac{R}{h_c}} \tan^{-1}\left(\frac{x_n}{\sqrt{Rh_c}}\right) +$$

$$(4\tau_y \sqrt{Rh_c} - 2\tau_y m_1 x_2 \sqrt{\frac{R}{h_c}}) \tan^{-1}\left(\frac{x_1}{\sqrt{Rh_c}}\right) - (4\tau_y \sqrt{Rh_c} + 2\tau_y m_2 x_2 \sqrt{\frac{R}{h_c}}) \tan^{-1}\left(\frac{x_1}{\sqrt{Rh_c}}\right)$$

24

The roll gap at neutral position h_n can be written as h_c plus x_n square by R . Normal pressure p is given by $p(x) = 2\tau_y - (\sigma_1 + \int_{x_1}^x \frac{2\tau_y}{h(x)} (\mp m - \frac{2x}{R}) dx)$. So, then the resultant sheet deformation force can be calculated f^s .

So, from this expression so you can calculate the trick this force resultant sheet deformation force. So, that is due to that is due to pressure and due to shear. So, both the things are there. So, due to pressure, so this is $p \times dx$ and then from for shear so this part is there. So, expanding this above equation so you can get the expression for f^s . So, this the purpose of this, this roll bite model is to find this force f^s this force f^s .

(Refer Slide Time: 22:35)

Results and Discussions

- Here case is considered when inlet strip thickness is 2.54 mm and initial position of upper work roll ' h_{c0} ' is 1.8mm. friction coefficients are set to be same in both backward and forward direction as $m_1=m_2=0.1$.
- initial conditions are $y_d=0.1\%$ of h_{c0} and $y_d \dot{=} 0$

work roll mass =2299.98 Kg/m, strip shear yield strength of Al is 110 MPa, work roll and backup roll diameter are 0.61 and 1.52 m respectively. Friction coefficients equal to 0.1 and front and back tensions are less than 170 MPa. (less than yield strength of strip material)

MOOCS/IITG/ME/SKD/LEC35

25

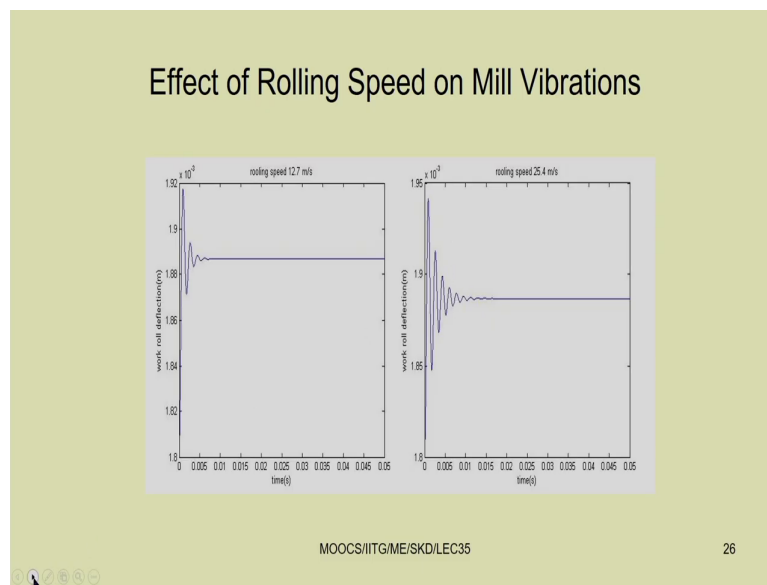
So, after getting this f_s now we can substitute it in the original equation that is $M d^2 y / dt^2 + K y = f_s$ and simulate that thing. So, we can use this Runge Kutta method to do that simulation or you can use the simulink model. And here it may be noted that several other models can also be developed to find the response.

So, initial condition initial y_d equal to taken 1 percent as h_{c0} and $y_d \dot{=} 0$ are taken to be 0 for the simulation. So, here in this case of numerical analysis when the inlet strip thickness is 2.54 mm, and the initial position of the upper roll is h_{c0} is 1.8 mm. So, friction coefficient are set to be same in both backward and forward direction that is m_1 equal to m_2 equal to 0.1 is considered.

Here the work roll mass is considered to be 2299.98 kg per meter, strip shear strength of aluminum is 110 MPa, work roll and backup roll diameters are 0.61 and 1.52 meter

respectively. Friction coefficients equal to 0.1 and ok, and the front and back tension are less than 170 MPa less than yield strength of the strip material. So, this back tension and this front and back tensions are taken to less than the yield stress of the strip material.

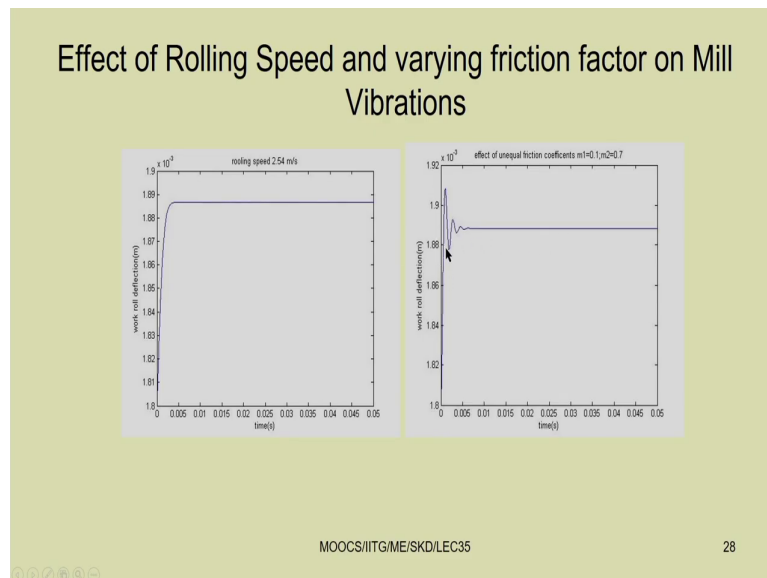
(Refer Slide Time: 24:13)



So, if you can simulate this thing then this work roll deflection that is y , you can see it is in this form. So, 1.92 into 10 to the power minus 2. So, that means, 1.92 mm. So, maximum. So, in the initial position you just see initially so there is some vibration. So, that is or the and it after sometimes it settle down.

So, but in this case when, so this is the speed is 12.7 meter per second. So, it settles down at 0.01 second, but if the speed is increased to 25.5. So, you just see so this amplitude is also increased and also the settling time is also increased. So, it has a greater settling time, so there will be some chatter mark on the tool.

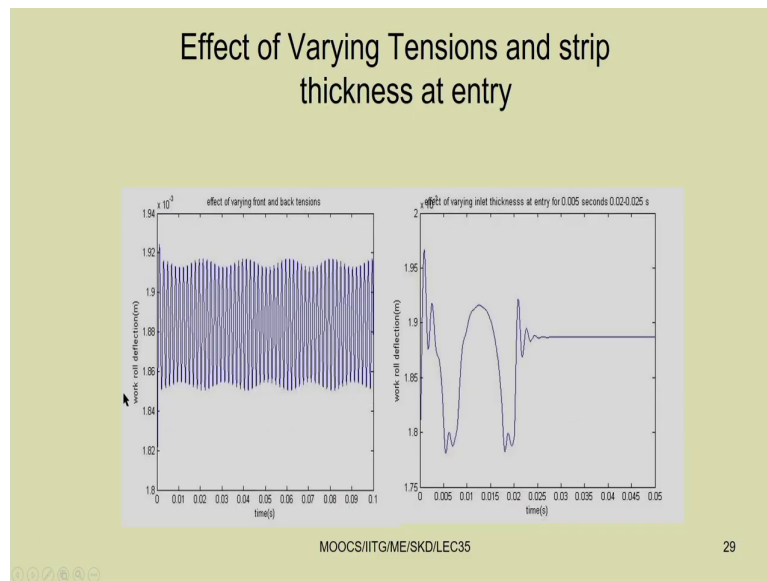
(Refer Slide Time: 25:12)



Similarly, it can be the effect of rolling speed and varying friction factor on the mill vibration can also be studied. So, rolling speed is 2.54 meter per second. So, this is you can see here the work roll reflection is less than this thing 2.54, previously you have taken more. And here we have taken the effect of one equal friction. So, it is taken this m_1 m_2 0.1 is taken. So, if you are taking this m_1 and m_2 , m_1 is 0.1 and m_2 equal to 0.7.

So, you can see that. So, here you just see so there is initially. So, there is no oscillations here, but in this case you can see some oscillation taking place so, but there is the initial roll gap is there. So, it will cover through this initial roll gap and there then it is smooth. But in this case so there is a initial deflection in the initial deflection is there.

(Refer Slide Time: 26:27)



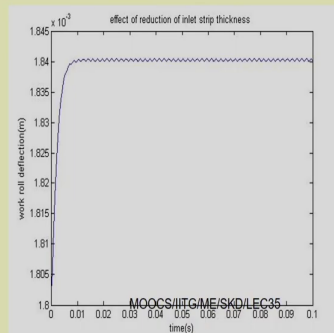
So, which will result in the result in the chatter mark in the sheet, and you can see more chatter mark you can get. So, effect of wiring the front and back tensions. So, by varying the front and back tension so you can see lot of oscillations occur or and due to that things some marks will be there.

And, so if the entry the inlet thickness at entry at point 0.05 second and 0.02 second so in this figure. So, it can be this some portion has been taken and plotted it here. So, you can see so there is lot of oscillations in the strip. So, due to these oscillations so there will be mark on chatter mark on the tool, mark chatter mark on the strip will be there.

(Refer Slide Time: 27:15)

Effect of Reduction of Strip Thickness up to 0.01 mm

Figure shows the system response for 0.01 mm strip entry thickness. It can be clearly seen that this friction factor model doesn't give good results for small entry thickness.



31

So, here you just see, though in previous case we have seen previous case we have seen there is less undulation or quickly it has reached to the that steady state response, but in this case the system response is 0.01 mm strip entry thickness. So, here effect of reduction of strip thickness.

So, if we have a very small strip 0.01 mm. So, in that case more oscillations will be there and clearly. So, it can be clearly seen that this friction factor model does not give good result for small entry thickness. So, if we have a small entry thickness, so in that case you can see this module is showing that always there will be a chatter mark in the strip.

(Refer Slide Time: 28:12)

REFERENCES

1. Roberts, E. Johnson, Quan Qi, 1993, "Chatter Dynamics in Sheet Rolling," Int. J. Mechanical Science, Vol-36, No-7, pp. 617-630
2. Chefneux, L., Fischbach, J.-P., and Gouzou, J., 1984, " Study and Industrial Control of Chatter in Cold Rolling," Iron and Steel Engineer, 61, November, pp. 17-26.
3. Yun, I. S., Wilson, W. R. D., Ehmaan, K. F., 1998, "Review of Chatter Studies in Cold Rolling," J. Machine Tool and Manufacturing, 38, pp. 1499-1530.
4. Yun, I. S., Wilson, W. R. D., Ehmaan, K. F., 1998, "Chatter in Strip Rolling Process-Part I: Dynamic Rolling Modeling," ASME, J. Manufacturing Science Engineering., pp. 330-336.

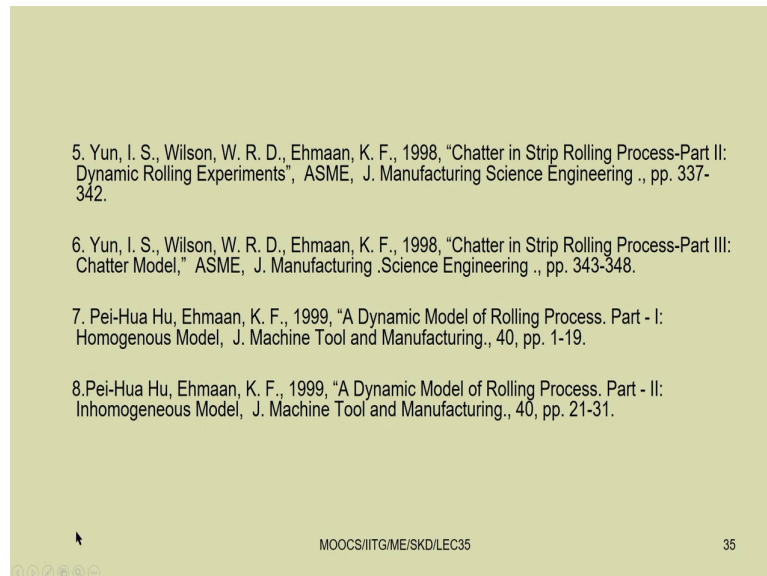
So, in this way one can do this analysis of a four high rolling mill. So, one can study other different type of rolling mills also. Also one can take this linear stiffness k to be non-linear and in that case the analysis will be different. So, there is several other roll bite models are available and some decent roll bite model studied by Sajan Kapil and Eberhard and myself. So, you can see those things. And all these are the references what we have seen in this work.

So, the references Robert and Johnson E Robert, Roberts E Johnson, Quan Qi. So, this is a old paper 1993. So, Chatter Dynamics in Sheet Rolling. So, International Journal of Mechanical Science. So, then you can see these paper Chefneux and Fischbach and Gouzou in 1984.

So, Study and Industrial Control of Chatter in Cold Rolling. So, Iron and Steel Engineers (Refer Time: 29:24) So, then Yun, so he has lot of paper in this field. So, Yun, Wilson and

Ehmann et al., 1988 review of Chatter Studies in Cold Rolling. Then Yun, Wilson and Ehmann, Chatter in Strip Rolling Process. So, part I and part II. So, they have two parts in this paper. So, dynamic rolling model. So, it is published in this ASME Journal of Manufacturing Science Engineering.

(Refer Slide Time: 29:51)



And then Yun, Wilson and Ehmann Chatter in Strip Rolling Process. So, part II. So, Dynamics Rolling. So, here experiment has been carried out. So, this is published in Jsm ASME Journal of Manufacturing Science Engineering.

Yun has several other paper also Yun, Wilson and Ehmann 1998; Chatter in Strip Rolling Process part III. So, chatter model. So, Ehmann has several other papers. Pei Hua Hu and Ehmann K F 1999; A Dynamic Model of Rolling Process part I Homogenous Model.

(Refer Slide Time: 30:30)

9. Kimura, Y., Sodani, Y., Nishiura, N., Ikeuchi, N., Mihara, Y., 2002, "Chatter Analysis in Tandem Cold Rolling Mills," Iron Steel Institute of Japan, Int., Vol.43 pp.77-84

10. Meehan, A. Paul, 2002, "Vibration Instability in Rolling Mills: Modeling and Experimental Results," ASME, J. of Vibration and Acoustics, Vol.124, pp. 221-228.

11. Farley, T. W. D., Rogers, S., Nardini, D., "Understanding Mill Vibration Phenomenon," Innoval Technology Limited, pp. 1-7.

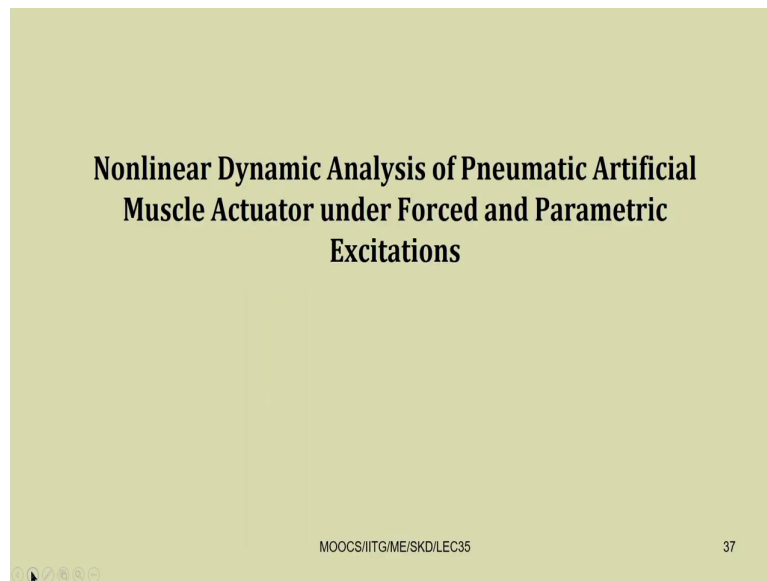
12. Lin, Y. J., Suh, C. S., Langari, R., Naoh, S. T., 2003, "On Characteristics and Mechanism of Rolling Instability and Chatter," ASME, J. Manufacturing Science Engineering., Vol.125, pp. 778-786.

MOOCS/IITG/ME/SKD/LEC35 36

And in part II, so they have these inhomogenous model studied. Then Kimura Sodani, Nishiura, Ikeuchi and Mihara. So, in 2002 Chatter Analysis in Tandem Cold Rolling Mill. So, there is a tandem mills, a number of rolling mills are there. So, in tandem rolling mills you can see this work. Then Meehan and Paul. So, Vibration Instability in Rolling Mills Modeling and Experimental Result.

So, then Farley and Rogers Farley, Rogers, and Nardini. So, Understanding Mill Vibration Phenomenon, Innoval Technology. So, this is a good paper so you can find this paper. So, Lin Langari Naoh. So, on characteristics and mechanism of rolling instability and chatter. So, this is also published in ASME Manufacturing Science Engineering. So, in 2003.

(Refer Slide Time: 31:32)



So, you can find several other papers in rolling mill and some recent papers also in rolling mills are there so, where you can study the rolling process. So, this way we have studied two manufacturing process and you have one is in toning operation, one is in this rolling operation actually.

So, this toning operation can be extended for milling operation and rolling operations also, and this forming this rolling operation can be informing operation. The basic idea is to or basic thing is to find a force. So, this force sometimes it is a non-linear force which is a function of the displacement of the sheet metal.

So, in that case it can be modeled as a parametrically excited system and considering this nonlinearity so we can have different resonance conditions. For example, we have studied principle parametric resonance conditions, combination resonance conditions and also in

addition to that in case of simple resonance conditions, we may have super harmonic and sub harmonic resonance conditions at different frequencies.

So, we can study all this type of vibration depending on the applications and in which range of frequency the system is operating. So, this way we can study the non-linear vibration of manufacturing systems. So, let us see some more electro mechanical systems; for example, so let us analyze now a pneumatic artificial muscle.

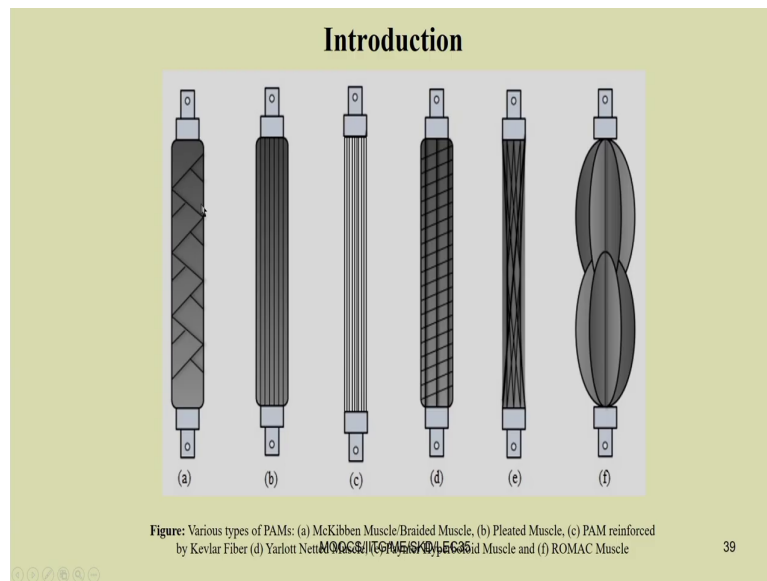
So, a pneumatic artificial muscle is used generally for actuators so pneumatic actuators. Pneumatic actuators can find many application, it can find applications in the rehabilitation process also, so or in this ex skeleton one can use this pneumatic actuator. So, in mechatronic systems either one can use a hydraulic system or pneumatic system.

Also one may use this motors so, electric motors where it may be, where it may be this DC motor AC motors, so also it may be this servo motors, stepper motor. So, depending on the motor and or depending on the these prime overs, so one can model the or one can dynamically model the systems.

And after modeling the system one can find the response of the system to study the system. So, always this dynamic model will be very very useful to study the dynamics of the system. So, now we are going to study the non-linear dynamics analysis of pneumatic artificial muscle actuator under force and parametric excitation.

So, already we have discussed what is force excitation. Particularly we tell about force excitation when the or force vibration of a system, so when the system is when the direction of the force and the response takes place in the same direction, but when they occur in perpendicular direction generally we talk regarding the parametrically excited system.

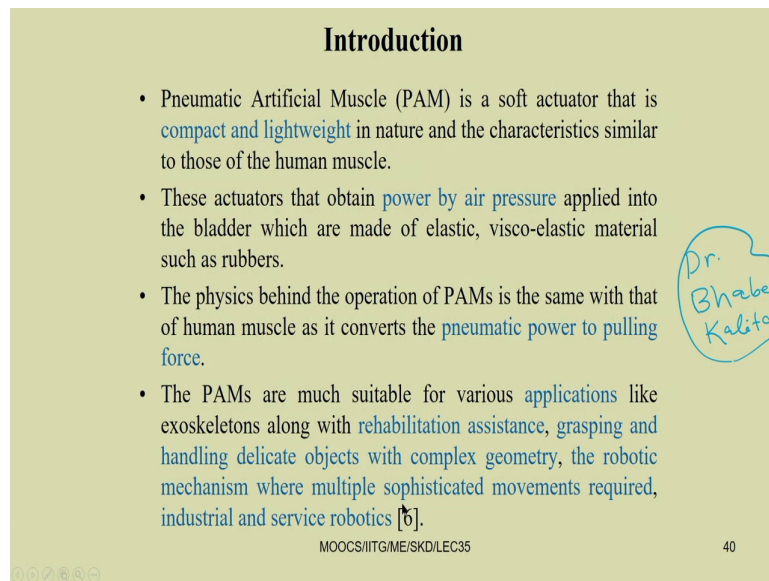
(Refer Slide Time: 34:59)



So, these are different type of various terms. So, the first one so we can see this is McKibben Muscle or Braided Muscle, then Pleated Muscles. So, we can see this pleated muscle, then we have PAM reinforce reinforce with Kevlar Fiber, then Yarlott Nett Muscles. Then, so there are several other muscles are there. So, these are several, these are the muscles actually used in several applications.

So, here we have to apply this pneumatic force or here we have to introduce into these graded muscles. So, due to the air force so this will expand in the transverse direction and there will be a contraction in the longitudinal direction. So, due to this contraction or this contraction can be used for actuating this muscle. So, we have to provide this air force or pneumatic force by either using a blower or compressor and we can actuate these muscles for different applications.

(Refer Slide Time: 36:18)



Introduction

- Pneumatic Artificial Muscle (PAM) is a soft actuator that is compact and lightweight in nature and the characteristics similar to those of the human muscle.
- These actuators that obtain power by air pressure applied into the bladder which are made of elastic, visco-elastic material such as rubbers.
- The physics behind the operation of PAMs is the same with that of human muscle as it converts the pneumatic power to pulling force.
- The PAMs are much suitable for various applications like exoskeletons along with rehabilitation assistance, grasping and handling delicate objects with complex geometry, the robotic mechanism where multiple sophisticated movements required, industrial and service robotics [6].

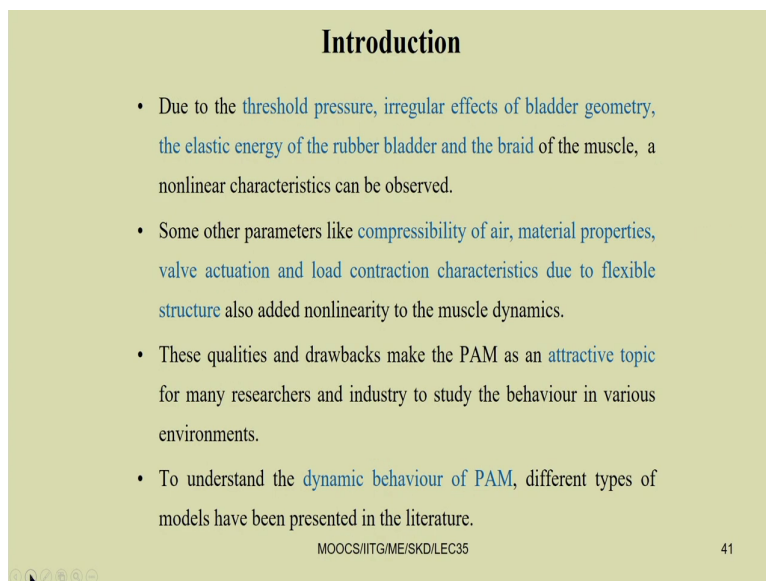
MOOCS/IITG/ME/SKD/LEC35 40

So, this pneumatic artificial muscle, so actually this work is part of the PhD work of my PhD student. So, now, he has defended his thesis. So, he is Dr. Bhaben Kalita. So, this is the part of the work by Dr. Bhaben Kalita who was my PhD student. So, here this pneumatic artificial muscle is a soft actuator, so that is compact and lightweight in nature and the characteristics similar to those of the human muscle.

So, these actuators are obtained power by air pressure, applied into the bladder which are made of elastic viscoelastic material such as rubber. So, the physics behind the operation of PAM is the same with that of human muscle as it converts pneumatic power into pulling force. So, here in case of the human so we are for example, in our hand we use our triceps and biceps to actuate the hand motion.

Similarly, here by putting this pneumatic force, so we can achieve this pulling or pushing action. So, the PAMs are much suitable for various applications like exoskeleton along the rehabilitation assistance, grasping and handling delicate objects with complex geometry, the robotic mechanism where multiple sophisticated movements required, industrial and service robotics also we can use.

(Refer Slide Time: 37:55)



Introduction

- Due to the threshold pressure, irregular effects of bladder geometry, the elastic energy of the rubber bladder and the braid of the muscle, a nonlinear characteristics can be observed.
- Some other parameters like compressibility of air, material properties, valve actuation and load contraction characteristics due to flexible structure also added nonlinearity to the muscle dynamics.
- These qualities and drawbacks make the PAM as an attractive topic for many researchers and industry to study the behaviour in various environments.
- To understand the dynamic behaviour of PAM, different types of models have been presented in the literature.

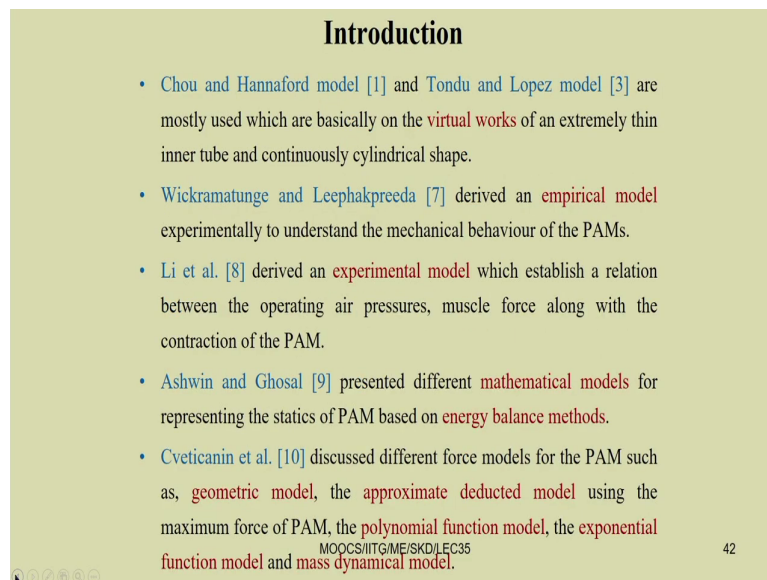
MOOCS/IITG/ME/SKD/LEC35 41

So, due to the threshold pressure, irregular effect of bladder geometry, the elastic energy of the rubber bladder and the braid of the muscle, a non-linear characteristics can be observed. Some of the some other parameters like this compressibility of air, material properties, valve actuation and load contraction characteristic due to flexible structure also added nonlinearity to the muscle dynamics.

So, these qualities and drawbacks make the PAM, as an attractive topic for many researchers and industry to study various behavior of the PAM in different applications or different environments. To understand the dynamics behavior of PAM different types of models have been presented in literature.

So, experimentally generally these material characteristics of the PAMs are first derived and then this actuation force in terms of different muscle contraction and muscle parameters have been developed by different researchers.

(Refer Slide Time: 39:11)



Introduction

- Chou and Hannaford model [1] and Tondur and Lopez model [3] are mostly used which are basically on the **virtual works** of an extremely thin inner tube and continuously cylindrical shape.
- Wickramatunge and Leephakpreeda [7] derived an **empirical model** experimentally to understand the mechanical behaviour of the PAMs.
- Li et al. [8] derived an **experimental model** which establish a relation between the operating air pressures, muscle force along with the contraction of the PAM.
- Ashwin and Ghosal [9] presented different **mathematical models** for representing the statics of PAM based on **energy balance methods**.
- Cveticanin et al. [10] discussed different force models for the PAM such as, **geometric model**, the **approximate deducted model** using the maximum force of PAM, the **polynomial function model**, the **exponential function model** and **mass dynamical model**.

MOOCs/IITG/ME/ISKO/LEC35

42

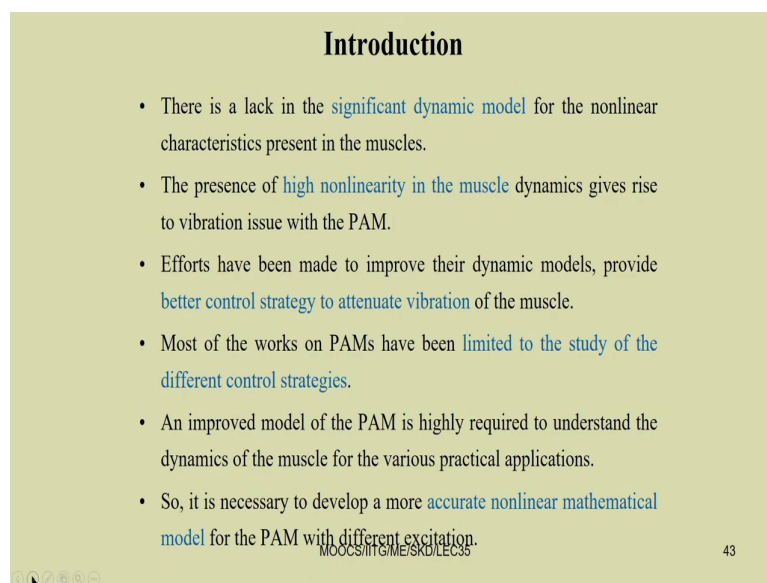
So, we will see all those. So, some of the literature are by this Chou and Hannaford and Tondur and Lopez. So, mostly used basically virtual work and of an extremely thin inner tube

and continuously cylindrical shape artificial muscle. Wickramatunge and Leephakpreeda, so they derived empirical model experimentally to understand the mechanical behavior of PAM.

Li et al derived experimental model which establish a relation between the operating air pressure, muscle force along with the contraction of the PAM. So, here in this work we followed this expression of Li et al and we have conducted our own experiments also to characterize the PAM.

So, Ashwin and Ghosal presented different mathematical models for representing the statics are of PAM based energy balance method. So, there are several others researchers worked in this field.

(Refer Slide Time: 40:17)



Introduction

- There is a lack in the significant dynamic model for the nonlinear characteristics present in the muscles.
- The presence of high nonlinearity in the muscle dynamics gives rise to vibration issue with the PAM.
- Efforts have been made to improve their dynamic models, provide better control strategy to attenuate vibration of the muscle.
- Most of the works on PAMs have been limited to the study of the different control strategies.
- An improved model of the PAM is highly required to understand the dynamics of the muscle for the various practical applications.
- So, it is necessary to develop a more accurate nonlinear mathematical model for the PAM with different excitation.

MOOCs@IITG/ME/SKD/LEC35 43

And you can find lot of work related to this pneumatic artificial muscle.

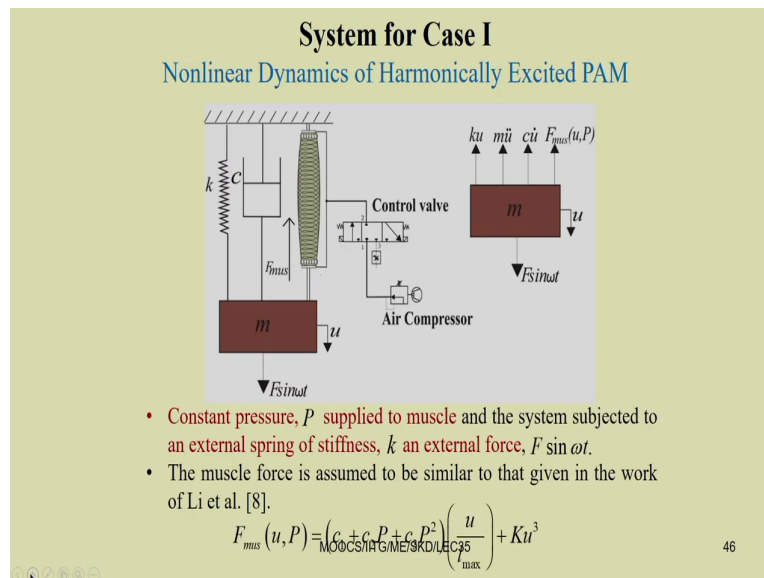
(Refer Slide Time: 40:21)

Objective of the Present Work

Along with these five cases, the following sub-objective of the proposed work are performed.

- Determination of the safe operating range of the different active and passive parameters of the PAM.
- Design and development of experimental setup to investigate the dynamics of the PAM.
- The theoretical observations have been compared with those obtained from the experimental work using a McKibben Muscle.
- A new type of PAM has been manufactured with the locally available fabrics and silicon rubber.

(Refer Slide Time: 40:26)



So, now, I am going to show you two or three models. So, the first model is non-linear dynamics of harmonically excited PAM. So, here I will show you both experimentally and theoretically how this equation of motion, how this artificial muscle work and let us see this first model.

So, this is here we are going to study the non-linear dynamics of harmonically excited PAM. So, let us consider, so this is a PAM artificial muscle, pneumatic artificial muscle. So, this pneumatic artificial muscle you just see, so entry and exit. So, you can see, so it is this from air compressor this air is going through a control valve.

So, from this control valve this put inside this muscle so that it can contract. So, when it is contracting so you just see this side we have a spring also and spring and damper. So, this

spring and damper. So, initially let us have a spring damper system. So, already you are familiar with a spring damper system.

So, now by putting this artificial muscle or this pneumatic actuator, so we have to actuate this muscle force. So, let us apply force $F \sin \omega t$ to the system and our objective is to move these mass by applying this force. So, now the equation of motion can be written. So, here also we have added the inertia force.

So, inertia force is shown here. So, the spring force $k u$ inertia force $m \ddot{u}$ and damping force \dot{u} , and this muscle force F_{muscle} . And this is the excitation force acting on the muscle that is $F \sin \omega t$. So, here this muscle force actually is characterized by the, so it will be different for different type of muscles depending on the muscle material, depending on the braid of the muscles and different other parameters.

So, this F_{muscle} will be different and it is a function actually of the contraction u and also this pressure P . So, this muscle force can be retain u , P , $f_{\text{muscle}}(u, P)$ can be written as $c_1 + c_2 P + c_3 P^2 + K u^3$. So, we have written this thing by using a non-linear term $K u^3$. And so here; that means, we have taken four parameters; one is c_1 , c_2 , c_3 and K .

So, four parameters to represent this muscle force. So, this force parameter four parameters c_1 , c_2 , c_3 and K can be obtained from the experiments by performing actual experiments. So, one can find this muscle parameters.

(Refer Slide Time: 43:42)

System Modeling

- The equation of motion which is obtained using **Newton's 2nd law**.

$$m\ddot{u} + ku + c\dot{u} + F_{ms} = F \sin \omega t$$

$$\ddot{u} + \left[\frac{k}{m} + \frac{(c_1 + c_2 P + c_3 P^2)}{m l_{max}} \right] u + \frac{c}{m} \dot{u} + \frac{K}{m} u^3 = \frac{F}{m} \sin \omega t$$
- The **fundamental natural frequency**, $\omega_0 = \sqrt{\frac{k}{m} + \frac{(c_1 + c_2 P + c_3 P^2)}{m l_{max}}}$
- The **nondimensional displacement**, $x = u / r$ is used with a scaling factor r . A **non-dimensional time** $\tau = \omega_0 t$ is considered.
- The **book keeping parameter**, ε is less than 1 and the other following **nondimensional parameters** are used.

$$\Omega = \frac{\omega}{\omega_0}, \quad \mu = \frac{c}{2\varepsilon m \omega_0}, \quad \alpha = \frac{r^2 K}{\varepsilon m \omega_0^2}, \quad f = \frac{F}{r \varepsilon m \omega_0^2}$$

MOOCs/IITG/ME/SKD/LEC35 47

So, now so you just see these equation of motion can be written mu double u mu double dot plus ku plus cu dot plus F muscle equal to F sin omega t, or it can be written by substituting this value of F muscle and dividing this m it can be written u double dot plus k by m plus c 1 plus c 2 P plus c 3 P square by m l max into u plus c by m u dot plus K by mu cube equal to F by m sin omega t.

So, u is the displacement. So, here you can see. So, the coefficient of u can be taken as the natural frequency of the system. So, here omega 0 the constant, so this is a constant part. So, here you can take this as a constant part sometimes we can take this P to be a function of. So, p can be varying with time.

So, in that case it cannot be constant. So, this constant part coefficient of u can be taken as this omega 0 square. So, that is why this omega 0 equal to root over k by m plus c 1 plus c 2 P

plus $\frac{c}{3} \frac{P^2}{m l \max}$. So, you can notice that this natural frequency of the system, we can vary by changing this muscle pressure. So, by changing this pressure P . So, we can actively control the frequency of oscillation.

So, as you know by controlling this frequency of, so this natural frequency we can always avoid the resonance frequency or the resonance frequency can be away from the natural frequency, so that the resonance condition can be avoided. Or whenever we required we can control this muscle pressure and we can bring it to the resonance condition, so that we can have maximum displacement.

So, in this artificial muscle case we require the displacement to be more. So, as we require the displacement to be more, so that it can take more load or it can displace it more. So, in that case we have to operate near the resonance condition. So, we have to change this value of ω_0 by actively changing this pressure which we can supply from outside and we can control the motion of the system.

So, the non-dimensional displacement x we can take now this thing we can modify and we can take this x equal to u by r . So, r is used as a scaling. So, here r is used as a scaling factor. So, a non-dimensional time τ also can be taken as $\omega_0 t$. So, by taking this non-dimensional time $\omega_0 t$.

So we can write down this equation motion in a more simplified form, that is why this non-dimensional time is used. Also one can use this book keeping parameter. So, ϵ , so which is very very less than 1. So, write down this equation of motion in a better form where we can apply this perturbation method to solve this equation.

So, here we are taking this ω equal to ω by ω_0 . So, this ω is the external frequency and ω_0 is the natural frequency we have taken. So, μ we have taken equal to $\frac{c}{2 \epsilon m \omega_0}$, and α equal to $\frac{r^2 K}{\epsilon m \omega_0^2}$, f equal to $\frac{F}{\epsilon m \omega_0^2}$.

(Refer Slide Time: 47:40)

Harmonically Excited PAM

- The **temporal equation of motion** can be written as follows.

$$\frac{d^2x}{d\tau^2} + 2\varepsilon\mu \frac{dx}{d\tau} + x + \varepsilon\alpha x^3 = \varepsilon f \sin \Omega \tau$$
- The system is considered to be **harmonically excited** which undergoes **simple resonance condition**, $\Omega \approx 1$.
- By using the **second order MMS**, the reduced equations can be written as follows.

$$\frac{da}{dt} = \varepsilon \left(-\frac{f}{2} \cos \gamma - \mu a \right) + \frac{\varepsilon^2 (1+2\mu)}{2} \left(\frac{f}{2} \sin \gamma - \frac{3}{8} \alpha a^3 \right)$$

$$a \frac{d\gamma}{dt} = a \varepsilon \sigma - \left[\varepsilon \left(-\frac{f}{2} \sin \gamma + \frac{3}{8} \alpha a^3 \right) + \frac{\varepsilon^2 (1+2\mu)}{2} \left(-\frac{f}{2} \cos \gamma - \mu a \right) + \varepsilon^2 \frac{3\alpha^2 a^5}{256} \right]$$
- In the reduced equations, a and γ represents the **amplitude and phase of the response**.

MOOCS/IITG/ME/SKD/LEC35 48

So, writing this way you just see the equation now is converted to a better form is well known to you so which is similar to that of a duffing equation. So, this is d^2x by $d\tau^2$ plus $2\varepsilon\mu$ dx by $d\tau$ plus x plus $\varepsilon\alpha x^3$ equal to $\varepsilon f \sin \Omega \tau$.

So, you just see so you have make the system in such a way that the forcing is weak nonlinearity, forcing is of weak nonlinearity εf we have taken. So, if the forcing is very high then in that case this ε term will not be there. So, it can be $f \sin \Omega \tau$. So, in that case the excitation will be hard excitation.

So, here we are taking this cubic non-linear thing. So, cubic non-linear stiffness we have taken, so that is why this is $\varepsilon\alpha x^3$. And the damping viscous damping we have taken and the viscous damping we are considering it is of ε order and after write writing

down this equation of motion, so we can apply. So, there are several methods to solve this equation of motion this equation of motion.

So, the system is considered to be harmonically excited which undergoes simple resonance condition at ω equal to ω nearly equal to 1. So, here you just see the coefficient of x equal to 1 that is the natural frequency. So, as we have written it in non-dimensional form.

The non-dimensional natural frequency is 1, that is why this non-dimensional external frequency whenever it is nearly equal to 1, so we have the resonance condition and this resonance condition is the simple resonance condition. So, by using second order method of multiple scale, the reduced equation can be written as.

So, it can be written. So, $\frac{da}{dt}$ equal to $\epsilon \sin \gamma - \frac{f}{2} \cos \gamma - \mu a$ plus $\epsilon^2 \frac{1}{2} \sin \gamma + \frac{f}{2} \cos \gamma - \frac{3}{8} \alpha a^3$.

And $a \frac{d\gamma}{dt}$ equal to $\epsilon \cos \gamma - \frac{f}{2} \sin \gamma + \frac{3}{8} \alpha a^3$ plus $\epsilon^2 \frac{1}{2} \cos \gamma - \frac{f}{2} \sin \gamma - \frac{3}{8} \alpha a^3$ plus $\epsilon^3 \frac{1}{2} \sin \gamma + \frac{f}{2} \cos \gamma - \frac{3}{8} \alpha a^3$. So, as you know for steady state a and γ will not be function of t , so the left hand side will be equal to 0.

(Refer Slide Time: 50:36)

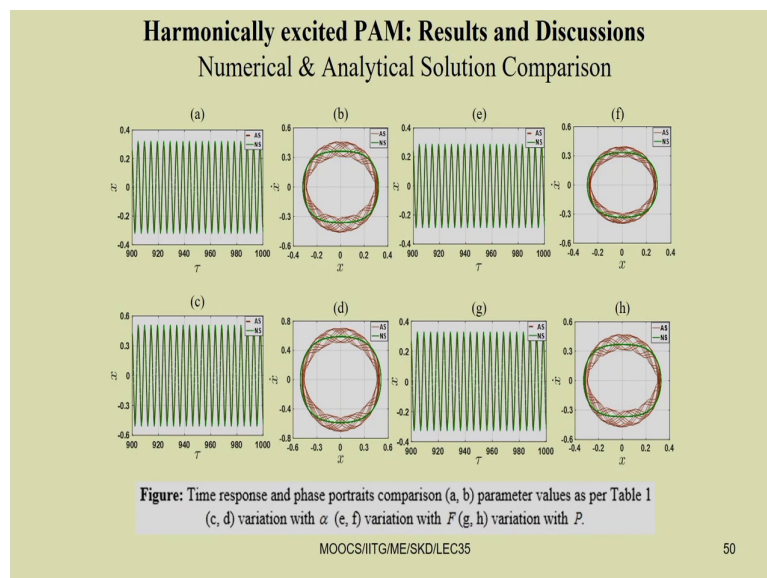
System Parameter Values for Case I

- The different system parameter values used in the study of numerical simulation.

Parameter	Numerical Value	Parameter	Numerical Value
l_{\max}	74 mm	m	6 N
c_1	-234.25 N	ε	0.1
c_2	1.96 N/kPa	P	500 kPa
c_3	-0.003 N/kPa ²	F	2 kN
α	150	k	12 N/mm
μ	0.01	r	1

So, now we can have a closed form solution and we can solve that closed form solution to find the response of the system. So, here these are the, so by performing experiments actually we got this parameter c_1 c_2 c_3 α μ , taking this l_{\max} equal to 74 mm. So, all these parameters have been obtained, so other parameters what are taken are here.

(Refer Slide Time: 51:05)

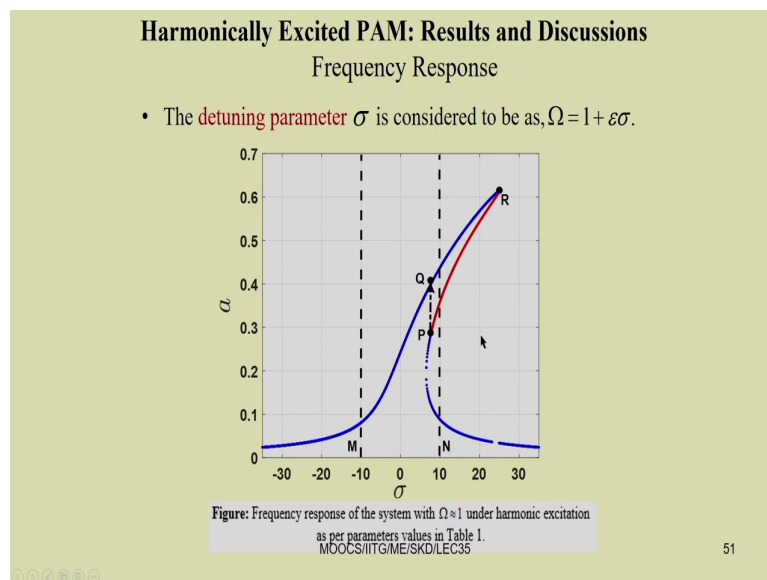


50

So, by taking all these parameters, so it is modeled and you can see the response. So, initially they have there is a comparison between the response obtained from this method of multiple scale and by solving this original equation using this Runge Kutta method.

So, we can see so there is a, so it is closely matching, so both the. So, this is numerical solution and this thing is closely matching. So, from the time response and the phase portrait you can see this method of multiple scale is giving close response.

(Refer Slide Time: 51:42)



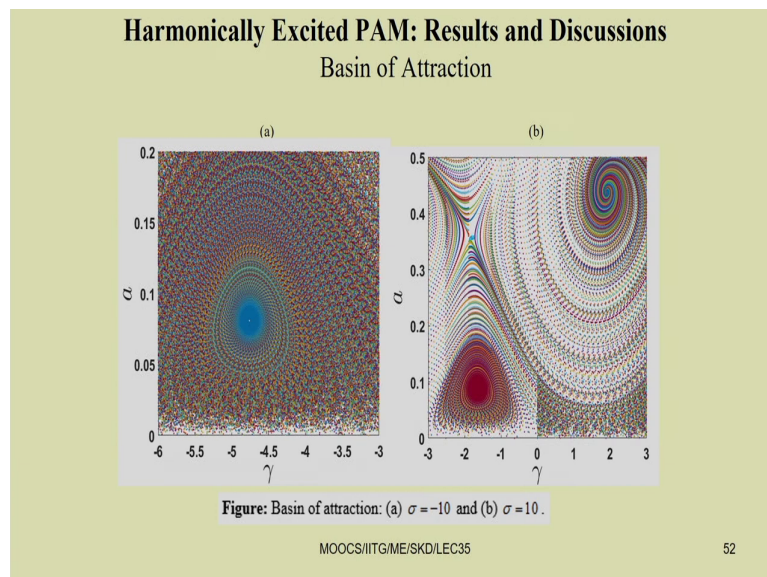
So, the advantage of using this method of multiple scale is that. So, now, we can plot the frequency response plot. So, this is the frequency response plot. So, in these numerical way so, if you are going to view this Runge Kutta method to solve or to find this frequency response plot you just see.

So, you have to solve that equation for here; for example, you have take more than 1000 points. So, at 1000 value of sigma you have to solve that equation using this Runge Kutta method, and then you require a huge memory space to store those 1000 data and from data from those data, again you have to find this steady state value of a to plot this response.

So, but by using this closed form solution what we have obtained. So, you can find this frequency response with a fraction of second, but you may required use computational time. So, if you are using this Runge Kutta method to find this frequency response ok.

So, here again you just see. So, this is a stable branch and this is unstable branch, and here we have a saddle node bifurcation or here other we can have a Hopf bifurcation and here we have a saddle node bifurcation. So, at this point so if we are reducing the frequency so you can see the system can jump from here to here.

(Refer Slide Time: 53:25)



So, it can jump from here to that point. So, if we are taking two points. So, you just see here at M so we have only one response, but if you are taking a point at N so you can see. So, we have three response are there so two stable and one unstable response is there. So, to get to

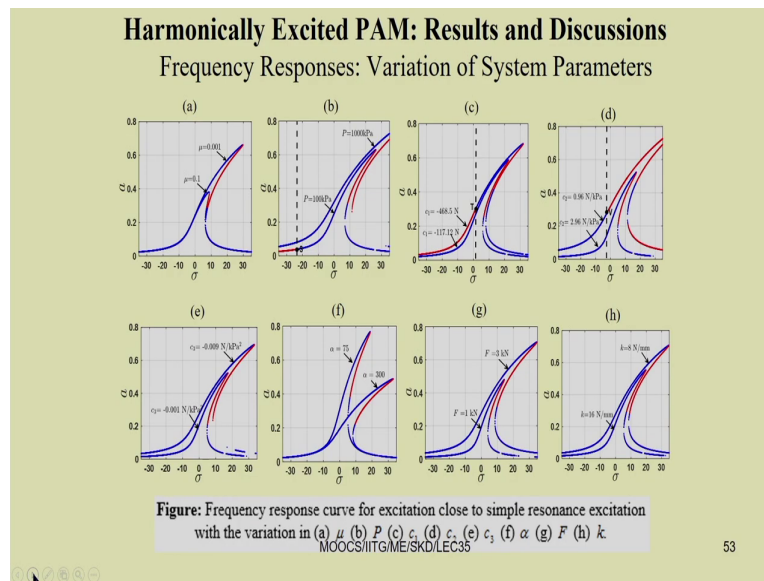
which stable or unstable response the system is moving so we have to plot the basin of attraction. So, the basin of attraction is plotted here.

So, at M_1 you can see that M_1 M point what you have shown. So, you have only one response. So, here A can be found less than 0.1. So, that thing clearly you can visualize here. So, this is the A value you are getting at the frequency at a σ so at a σ correspond to M_1 M and the other points.

So, you can see we are getting. So, this correspond to the saddle node point saddle node point and this correspond to. So, here clearly you can see so we have two stable response. So, all the branches or all the trajectories are moving to this point. here also all the trajectories from this basin. So, you just see from this basin all the trajectories are moving here. Here also from all the trajectories they are moving to this point.

So, if you are taking some initial condition from here so it will traverse to or travel to these point. And if you are taking some initial condition here, so you will get this stable response. And here so this actually you know this unstable point cannot be achieved with time, so it will take infinite time to reach this saddle node bifurcation point as this is unstable point.

(Refer Slide Time: 55:35)



So, either the response will go to this point or this point. So, this way you can find the basin of attraction. So, for different system parameter these things have been studied frequency response variation with the different system parameter.

For example, so in this case we have taken two value of μ that is damping. So, with damping it is reduced you can see, then with different pressure, so 1000 100 KPA and one thousand KPA. So, by applying this higher pressure you just see so this is the response plot and for the lower response. So, inside plot is for 100 KPA and outside plot is for higher KPA that is this kilo pascal pressure is applied here.

So, then muscle parameter c_1 c_2 . So, these are the muscle parameter for different muscle parameter. You know that the muscle parameter depends on the materials we are using. So, by using different materials so they can be changed. So, having different muscle parameters c

1 c 2, then this is c 3 and this is the nonlinearity, effect of nonlinearity you can see. So, this is alpha equal to 75.

So, this alpha equal to 300. So, then these are the forcing, amplitude of forcing 1 kilo newton 3 kilo newton. So, due to higher forcing the response amplitude is high and due to, so then this variation of K is also taken this non-linear term in this muscle force.

(Refer Slide Time: 57:17)

Harmonically Excited PAM: Results and Discussions
Application of the Developed Results

- To achieve an amplitude of $a = 0.35$, various set of system parameters are as follows.

Case	μ	P	c_1	c_2	c_3	α	F	k	σ
1	0.01	500	-234.25	1.96	-0.003	150	2	12	5.2
2	0.001	500	-234.25	1.96	-0.003	150	2	12	4.9
3	0.1	500	-234.25	1.96	-0.003	150	2	12	5.8
4	0.01	100	-234.25	1.96	-0.003	150	2	12	4.8
5	0.01	1000	-234.25	1.96	-0.003	150	2	12	1.8
6	0.01	500	-468.50	1.96	-0.003	150	2	12	4.1
7	0.01	500	-117.12	1.96	-0.003	150	2	12	5.2
8	0.01	500	-234.25	2.96	-0.003	150	2	12	5.8
9	0.01	500	-234.25	1.96	-0.009	150	2	12	3.9
10	0.01	500	-234.25	1.96	-0.001	150	2	12	5.8
11	0.01	500	-234.25	1.96	-0.003	75	2	12	1.2
12	0.01	500	-234.25	1.96	-0.003	300	2	12	13.2
13	0.01	500	-234.25	1.96	-0.003	150	1	12	6.2
14	0.01	500	-234.25	1.96	-0.003	150	3	12	3.8
15	0.01	500	-234.25	1.96	-0.003	150	2	8	3.8
16	0.01	500	-234.25	1.96	-0.003	150	2	16	5.6

55

So, due to that thing also it has been plotted. So, you can find, so this way you can find the different response and also you can apply it for a different application purpose.

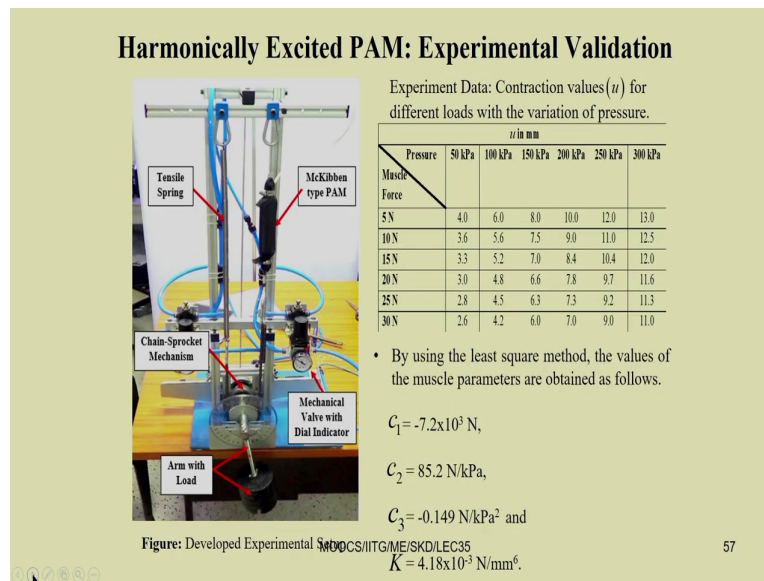
(Refer Slide Time: 57:27)

Harmonically Excited PAM: Results and Discussions			
Application of the Developed Results			
<ul style="list-style-type: none">Saddle node bifurcation point where maximum amplitude achieve for the studied PAM as below.			
Case	Variation of System parameters	a	σ
1	As per Table 1	0.61	24.9
2	$\mu = 0.001$	0.66	29.7
3	$\mu = 0.1$	0.38	8.7
4	$p = 100$	0.63	26.4
5	$c_1 = -458.50$	0.68	31.9
6	$c_1 = -117.12$	0.59	22.5
7	$c_2 = 2.96$	0.52	17.4
8	$c_3 = -0.009$	0.70	33.3
9	$c_3 = -0.001$	0.52	17.4
10	$\alpha = 75$	0.77	18.8
11	$\alpha = 300$	0.49	33
12	$F = 1$	0.48	14.3
13	$F = 3$	0.71	34.6
14	$k = 8$	0.71	34.7
15	$k = 16$	0.55	19.7

MOOCs/IITG/ME/SKD/LEC35

So, here we are not going to tell you in detail regarding this application purpose.

(Refer Slide Time: 57:31)



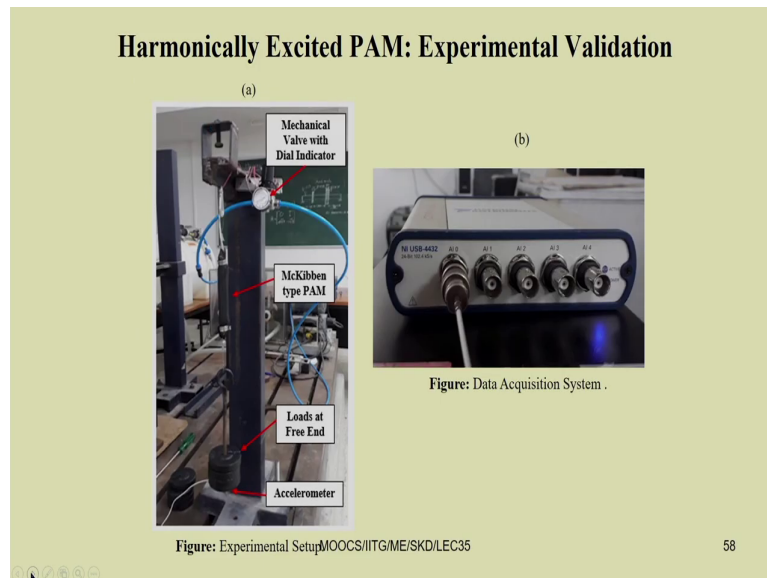
So, this is a machine developed to study the, so harmonically excited PAM. So, this is the this is the spring is connected here. So, this is the artificial muscle and this is the controller through which we can give the air pressure to the system. So, by taking this air pressure so the it is, here it is intended to rotate this or move this arm.

So, some load we have putted put here so we can see arm with load. So, here we have a rack and pinion system. So, when this pulley is moving, so it can move this rack and pinion. So, in turn, so it is connected to this arm and it will rotate this link.

So, this is particularly can be simulated or it can be mimic, it can mimic the motion of the arm. So, by putting this artificial muscle, so for paralytic or semi-paralytic person, so we can

move this arm. So, effectively we can use this muscle for the purpose of exoskeleton systems also.

(Refer Slide Time: 58:51)



So, you can see this is the. So, to characterize this thing so we have put the load and by giving different air pressure. So, we have seen so how much load it can take. So, single muscle.

(Refer Slide Time: 59:11)

Harmonically Excited PAM: Experimental Validation

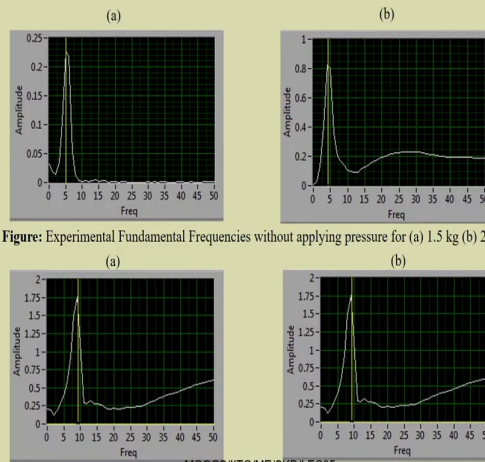


Figure: Experimental Fundamental Frequencies without applying pressure for (a) 1.5 kg (b) 2 kg.

Figure: Experimental Fundamental Frequencies for (a) 1.5 kg at 150 kPa (b) 2 kg at 200 kPa.

So, we can have different muscles also. So, these are the vibration of the muscles.

(Refer Slide Time: 59:16)

Harmonically Excited PAM : Experimental Validation

- Comparison of experimental and theoretical fundamental frequencies of the used McKibben muscle.

Case	Load	Pressure	Experimental Fundamental Frequency	Theoretical Fundamental Frequency
I	1.5 kg	150 kPa	9.1 Hz	8.0 Hz
II	2 kg	200 kPa	9.2 Hz	8.2 Hz

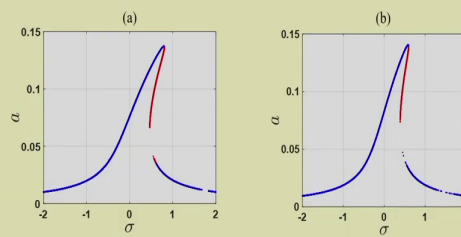
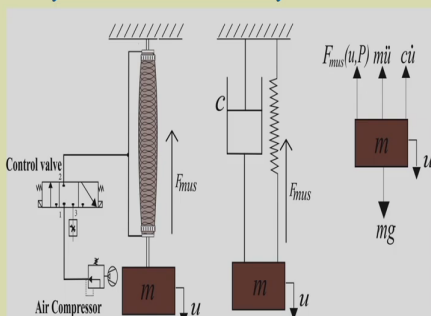


Figure: Frequency Response using experimentally obtained coefficients for the used McKibben muscle with 2 kg load at 200 kPa.

(Refer Slide Time: 59:24)

System for Case II

Dynamics of Parametrically Excited PAM



- Time varying pressure, $P = P_m + P_0 \sin \omega t$ supplied to muscle.
- The muscle force is assumed to be similar to that given in the work of Li et al. [8].

$$F_{mus}(u, P) = (c_1 + c_2 P + c_3 P^2) \left(\frac{u}{L_0} \right) + (d_1 + d_2 P)$$

MOOCS/IITG/ME/SKD/L6639

62

So, experimentally it is validated that it is giving these correct results. So, you can, so previously we have seen that thing as a force excited. So, now, we can consider these as a parametrically excited when we consider this P to be a function, time varying function of time varying function.

(Refer Slide Time: 59:42)

System Modeling

- The equation of motion which is obtained using **Newton's 2nd law**.

$$m\ddot{u} + c\dot{u} + F_{mus} - mg = 0$$

$$\ddot{u} + \left[\frac{(c_1 + c_2 P + c_3 P^2)}{m l_{max}} \right] \dot{u} + \frac{c}{m} \dot{u} + \left[\frac{(d_1 + d_2 P)}{m} - g \right] = 0$$
- The **fundamental natural frequency**, $\omega_0 = \sqrt{\frac{c_1 + c_2 P_m + c_3 \left(\frac{P_m^2}{2} + \frac{P_0^2}{2} \right)}{m l_{max}}}$
- The **nondimensional displacement**, $x = u / r$ is used with a scaling factor r . A **non-dimensional time** $\tau = \omega_0 t$ is considered.
- The **book keeping parameter**, ε is less than 1 and the other following **nondimensional parameters** are used.

$$\Omega = \frac{\omega}{\omega_0}, \mu = \frac{c}{2\varepsilon m \omega_0}, p_1 = \frac{c_2 P_0 + 2c_3 P_0 P_m}{\varepsilon m \omega_0^2 l_{max}}, p_2 = -\frac{c_3 P_0^2}{2\varepsilon m \omega_0^2 l_{max}},$$

$$f_1 = \frac{d_1 P_m + d_1 - mg}{\varepsilon m \omega_0^2}, f_2 = \frac{d_2 P_m}{\varepsilon m \omega_0^2}$$

So, here we can take these P. Similar, way we can analyze this system and here that P part we are taking it equal to P 0 plus P 1 cos omega t P can be taken as P m plus P 0 sin omega t.

So, here P is taken to be P m previous case we have taken P equal to P only, but here now we are adding a term that is P 0 sin omega t in this pressure. So, in that case the same equation we are taking that is F muscle equal to u P that is c 1 plus c 2 P plus c 3 P square into u by 1 plus d 1 plus d 2 P.

So, here we have taken a five parameter c 1 c 2 c 3 3 parameter and d 1 d 2, another 2 parameter. So, 5 parameter muscle parameter we have taken. So, this part is a function of u and this is independent of u. So, that is why we have taken two parts. So, now you can

observe this equation can be written as that of a parametrically excited system. So, you just see this is \ddot{u} . So, this part is a constant part in u .

(Refer Slide Time: 61:07)

Dynamics of Parametrically Excited PAM

- The temporal equation of motion is in the form of a forced and parametrically excited system as follows.

$$\frac{d^2 x}{d\tau^2} + 2\epsilon\mu \frac{dx}{d\tau} + \epsilon(1 + p_1 \sin \Omega\tau + p_2 \cos 2\Omega\tau)x = \epsilon(f_1 + f_2 \sin \Omega\tau)$$

- The system undergoes two resonance conditions and by using the second order MMS, the reduced equations can be written as follows.

- Simple resonance condition, $\Omega \approx 1$

$$a' = \frac{da}{dt} = \epsilon \left(-\frac{f_2}{2} \cos \gamma - \mu a - \frac{p_2 a}{4} \sin 2\gamma \right) + \frac{\epsilon^2(1+2\mu)}{2} \left(\frac{f_2}{2} \sin \gamma - \frac{p_2 a}{4} \cos 2\gamma \right) + \epsilon^2 \left(\frac{f_1 p_1}{4} \cos \gamma \right)$$

$$a\gamma' = a \frac{d\gamma}{dt} = a\epsilon\sigma - \left[\epsilon \left(-\frac{f_2}{2} \sin \gamma + \frac{p_2 a}{4} \cos 2\gamma \right) + \frac{\epsilon^2(1+2\mu)}{2} \left(-\frac{f_2}{2} \cos \gamma - \mu a - \frac{p_2 a}{4} \sin 2\gamma \right) \right. \\ \left. + \epsilon^2 \left[\frac{f_1 p_1}{4} \sin \gamma - \frac{p_1^2 a}{8(1-\epsilon^2\sigma^2)} + \frac{p_1^2 a}{8(1-\epsilon^2\sigma^2)} - \frac{p_2^2 a}{8(1-\epsilon^2\sigma^2)} \right] \right]$$

64

So, we will see ok. So, now, this is the equation, so simplified equation, $\frac{d^2 x}{d\tau^2} + 2\epsilon\mu \frac{dx}{d\tau} + \epsilon(1 + p_1 \sin \Omega\tau + p_2 \cos 2\Omega\tau)x = \epsilon(f_1 + f_2 \sin \Omega\tau)$. So, you just see the coefficient of x , so this part. So, 1 into x that is the constant part, but this other two that is $p_1 \sin \Omega\tau$ and $p_2 \cos 2\Omega\tau$ when they are coefficient of x . So, this leads to parametric excitation.

And in the right hand side also we have the forcing that is a constant part is that ϵf_1 plus $\epsilon f_2 \sin \Omega\tau$. So, here so, we can have different resonance conditions. So, by applying this method of multiple scales, so we can study different resonance conditions.

(Refer Slide Time: 61:56)

Dynamics of Parametrically Excited PAM

- Principal parametric resonance condition, $\Omega \approx 2$

$$a' = \frac{da}{dt} = \varepsilon \left(-\mu a + \frac{p_1}{4} a \cos 2\gamma \right) - \frac{\varepsilon^2 (1+2\mu)}{2} \left(\frac{p_1 a}{4} \sin 2\gamma \right) + \varepsilon^2 \left[\frac{p_1 p_2 a \cos 2\gamma}{8(1-(3+2\varepsilon\sigma)^2)} + \frac{p_1 p_2 a \cos 2\gamma}{8(1-(3+\varepsilon\sigma)^2)} \right]$$

$$a\gamma' = a \frac{d\gamma}{dt} = \frac{a\varepsilon\sigma}{2} \left[\frac{\varepsilon p_1 a}{4} \sin 2\gamma + \frac{\varepsilon^2 (1+2\mu)}{2} \left(-\mu a + \frac{p_1 a}{4} \cos 2\gamma \right) + \varepsilon^2 \left[-\frac{p_1^2 a}{8(1-(3+\varepsilon\sigma)^2)} \right. \right. \\ \left. \left. + \frac{p_1 p_2 a \sin 2\gamma}{8(1-(3+2\varepsilon\sigma)^2)} + \frac{p_1 p_2 a \sin 2\gamma}{8(1-(3+\varepsilon\sigma)^2)} - \frac{p_2^2 a}{8(1-(3+2\varepsilon\sigma)^2)} - \frac{p_2^2 a}{8(1-(5+2\varepsilon\sigma)^2)} \right] \right]$$

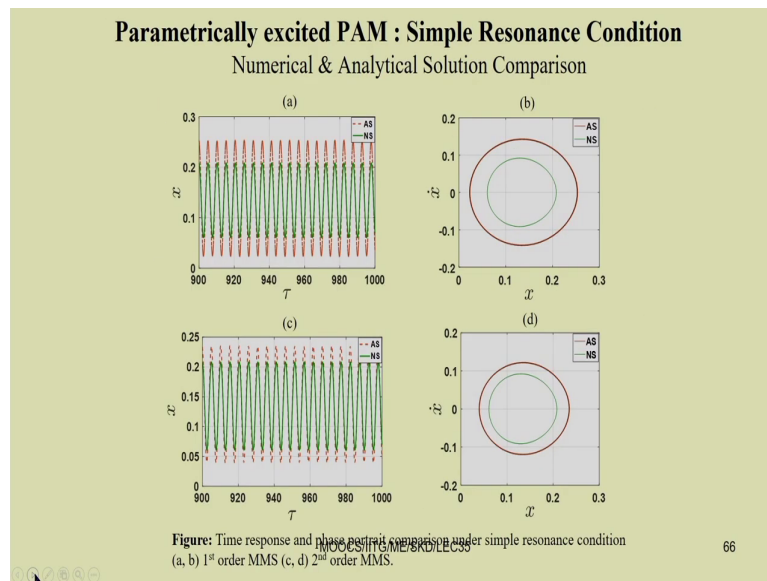
- The different system parameter values used in the study of numerical simulation.

Parameter	Numerical Value	Parameter	Numerical Value	Parameter	Numerical Value
l_{max}	74 mm	d_1	-100 N	P_0	58 kPa
c_1	-234.25 N	d_2	1 N/kPa	ε	0.1
c_2	1.96 N/kPa	m	6 N	μ	0.01
c_3	-0.003 N/kPa ²	P_m	300 kPa	r	1

MOOCS/IITG/ME/SKD/LEC35 65

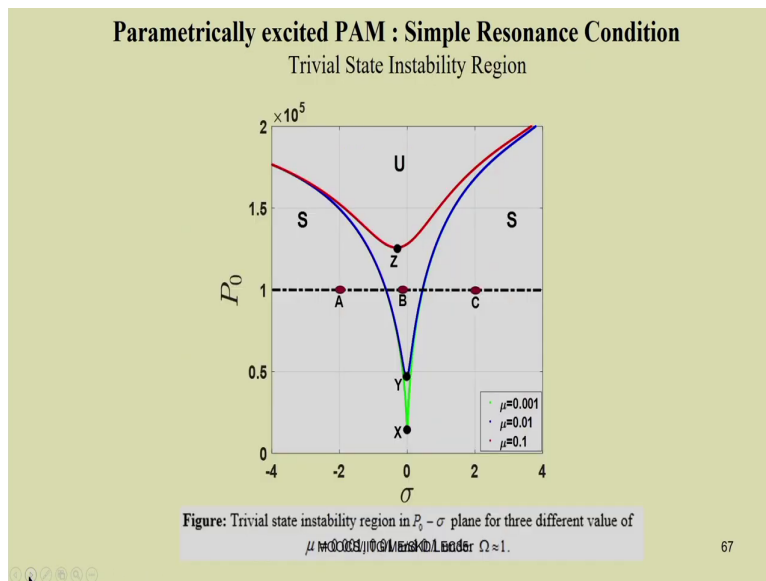
So, we can have this principle parametric resonance condition when omega nearly equal to 2.

(Refer Slide Time: 62:04)



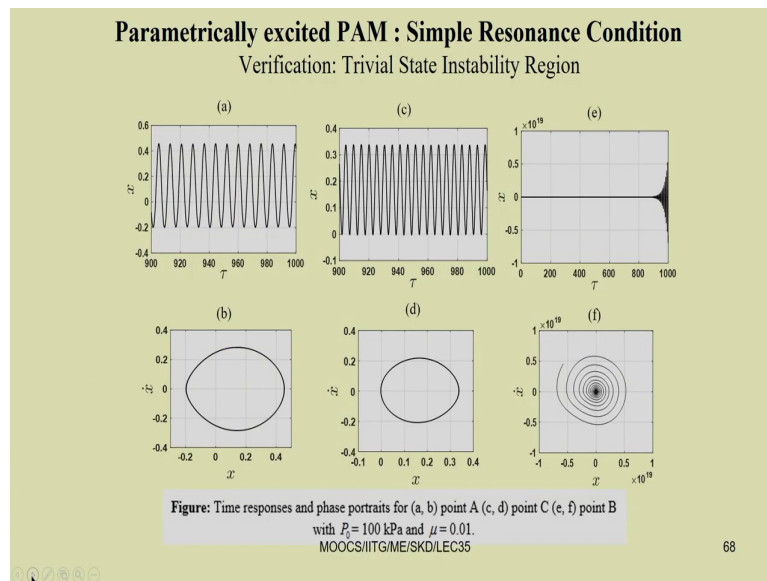
And, so in case of principle parametric resonance conditions again is numerical and analytical resonances have been plotted.

(Refer Slide Time: 62:13)



So, here you can see these parametric instability regions we have found. So, S is the region for where the system will be stable. That means, the muscle will not contract in this region where S is written. So, we have to operate the muscle in a region where it is U it is written U. So, that there will be some contraction in this muscle. So, if it is in the region S, so it will not contract and when it is in region U so it will contract.

(Refer Slide Time: 62:50)



So, by using this parametric instability region so, we can study different response of the system

(Refer Slide Time: 62:56)

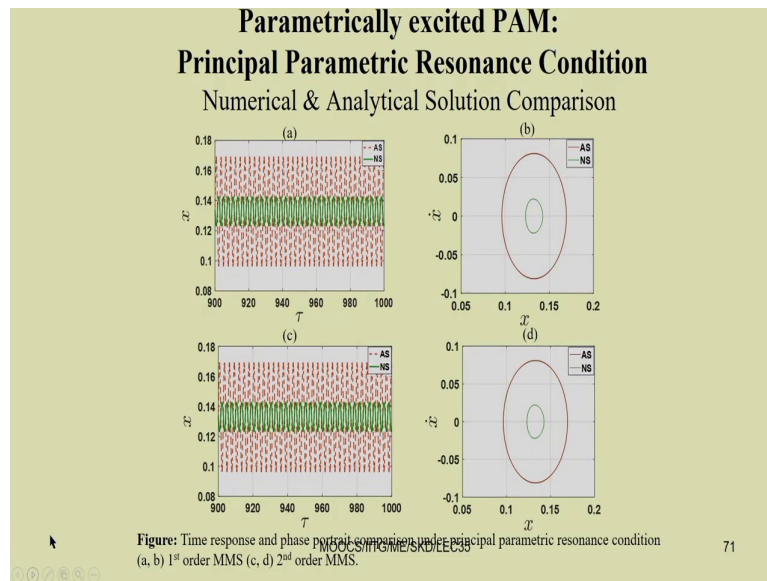
Parametrically Excited PAM : Simple Resonance Condition
Critical Value of Dynamic Pressure with Variation in System Parameter

Case	Variation in system parameter	P_{cr} (kPa)	σ
1	$c_1 = -117.12 \text{ N}$	71.8	-0.01
2	$c_1 = -234.25 \text{ N}$	46.5	-0.03
3	$c_1 = -468.50 \text{ N}$	64.7	-0.02
4	$c_2 = 2.96 \text{ N/kPa}$	99.2	-0.16
5	$c_2 = 1.96 \text{ N/kPa}$	46.4	-0.01
6	$c_2 = 0.96 \text{ N/kPa}$	77.5	-0.14
7	$c_3 = -0.001 \text{ N/kPa}^2$	142.4	-1.01
8	$c_3 = -0.003 \text{ N/kPa}^2$	46.4	-0.02
9	$c_3 = -0.009 \text{ N/kPa}^2$	65.0	-0.35
10	$d_1 = -50 \text{ N}$	46.4	-0.01
11	$d_1 = -100 \text{ N}$	46.4	-0.01
12	$d_1 = -200 \text{ N}$	46.4	-0.01
13	$d_2 = -2 \text{ N/kPa}$	46.4	-0.01
14	$d_2 = -1 \text{ N/kPa}$	46.4	-0.01
15	$d_2 = -0.5 \text{ N/kPa}$	46.4	-0.01
16	$P_n = 400 \text{ kPa}$	42.3	-0.12
17	$P_n = 300 \text{ kPa}$	46.5	-0.03
18	$P_n = 200 \text{ kPa}$	31.1	-0.72

70

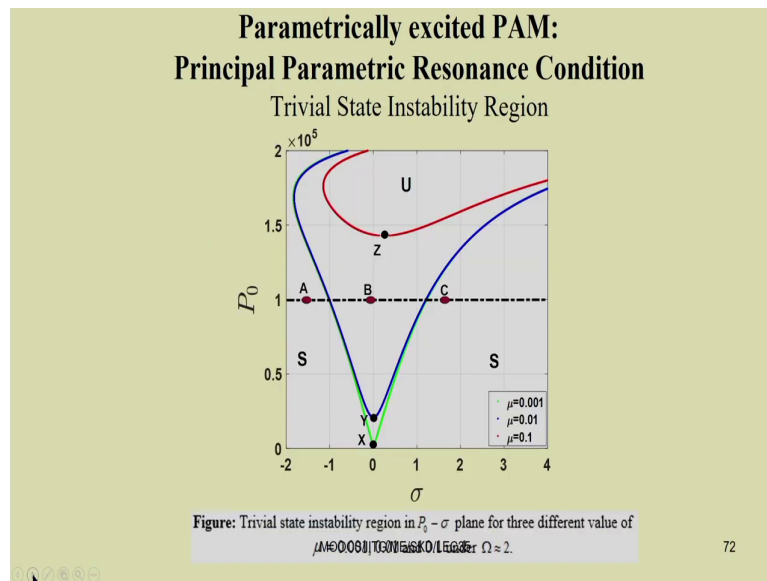
So, these are the instability region for different purposes, we can one can study this thing ok.

(Refer Slide Time: 63:02)



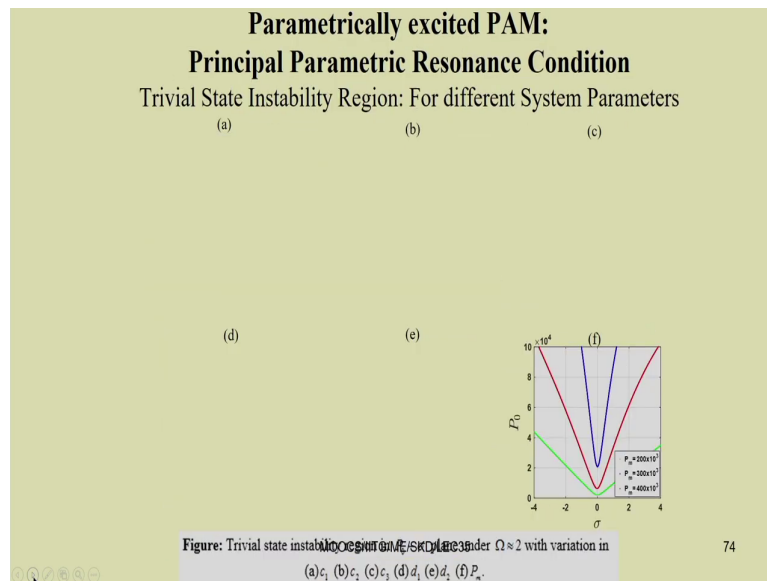
So, this is for principle parametric resonance, some comparisons are been here ok.

(Refer Slide Time: 63:09)



So, this is principle parametric resonance, trivial state instability region have been plotted and this verifications have been carried out.

(Refer Slide Time: 63:16)



(Refer Slide Time: 63:18)

Parametrically excited F.A.M.

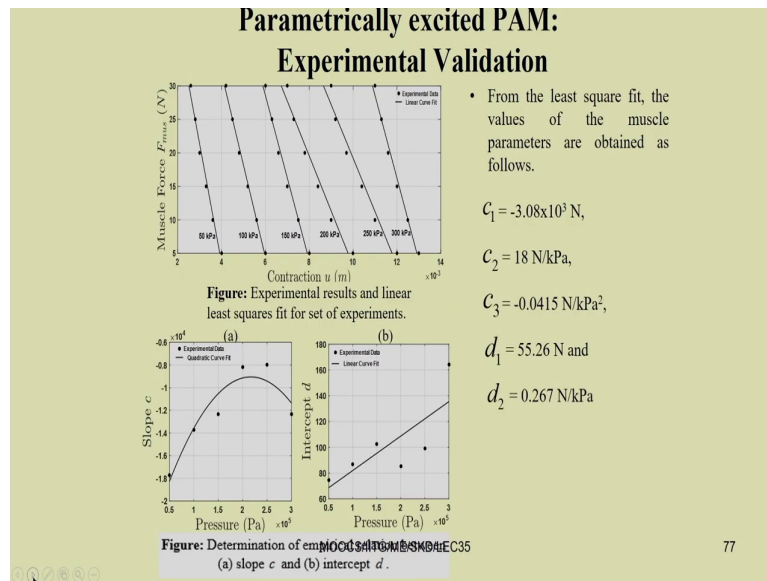
Principal Parametric Resonance Condition

Critical Value of Dynamic Pressure with Variation in System

Case	Variation in system parameter	Parameter P_{nc} (kPa)	σ
1	$c_1 = -117.12 \text{ N}$	49.5	0.02
2	$c_1 = -234.25 \text{ N}$	20.8	0.01
3	$c_1 = -468.50 \text{ N}$	38.2	-0.03
4	$c_2 = 2.96 \text{ N/kPa}$	13.3	-0.02
5	$c_2 = 1.96 \text{ N/kPa}$	20.8	0.01
6	$c_2 = 0.96 \text{ N/kPa}$	10.4	0.03
7	$c_3 = -0.001 \text{ N/kPa}^2$	7.8	-0.02
8	$c_3 = -0.003 \text{ N/kPa}^2$	20.8	0.01
9	$c_3 = -0.009 \text{ N/kPa}^2$	5.4	-0.03
10	$d_1 = -50 \text{ N}$	20.8	0.01
11	$d_1 = -100 \text{ N}$	20.8	0.01
12	$d_1 = -200 \text{ N}$	20.8	0.01
13	$d_2 = -2 \text{ N/kPa}$	20.8	0.01
14	$d_2 = -1 \text{ N/kPa}$	20.8	0.01
15	$d_2 = -0.5 \text{ N/kPa}$	20.8	0.01
16	$P_n = 400 \text{ kPa}$	6.4	0.01
17	$P_n = 300 \text{ kPa}$	20.8	0.01
18	$P_n = 200 \text{ kPa}$	2.0	0.03

75

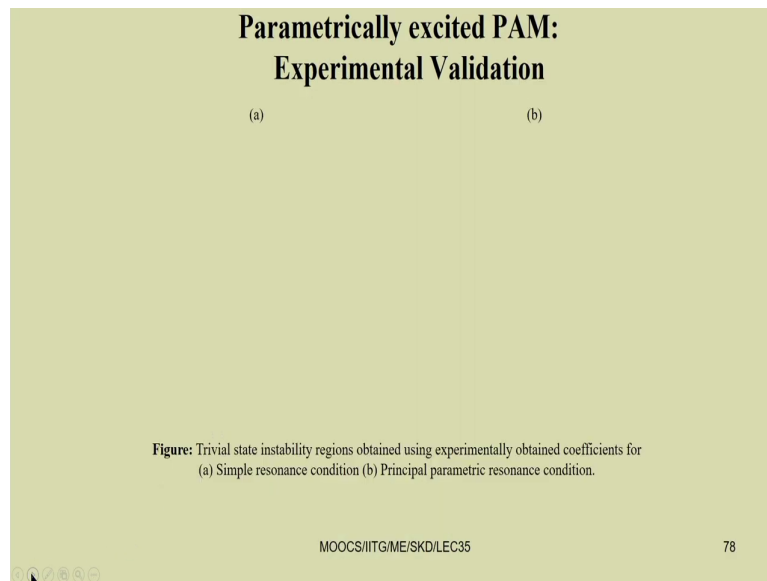
(Refer Slide Time: 63:19)



Similarly, this experimental verification have been carried out. So, to so this is this experiment, this muscle force versus the contraction U you have seen the experiments we have performed where we got different muscle force versus the contraction. So, for different pressure, so these things have been plotted.

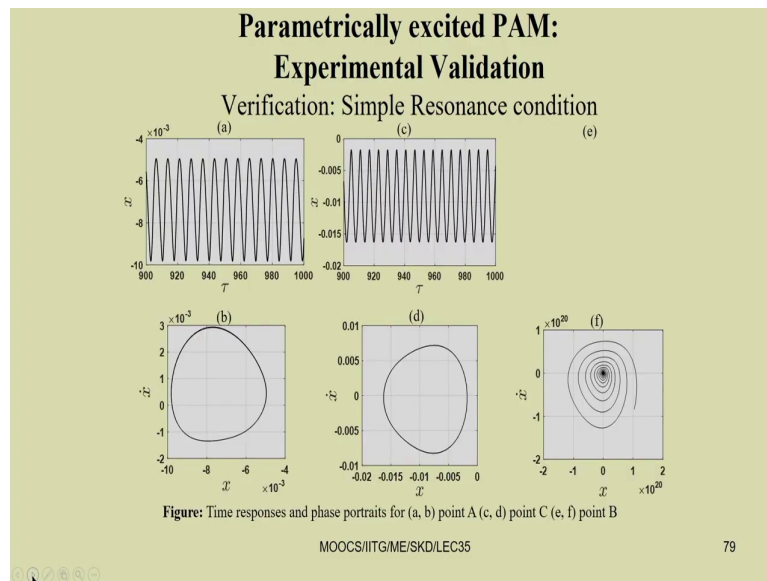
So, this for example, this 50 KPA this is 100 KPA this is 150 KPA. So, this is the muscle force. So, taking these things so we can obtain these c_1 c_2 c_3 d_1 d_2 from this experimental value. And, so initially we can put a. So, we can put a linear curve to find this slope of that curve, and from that things, so we can get some parameter c c_1 c_2 .

(Refer Slide Time: 64:15)

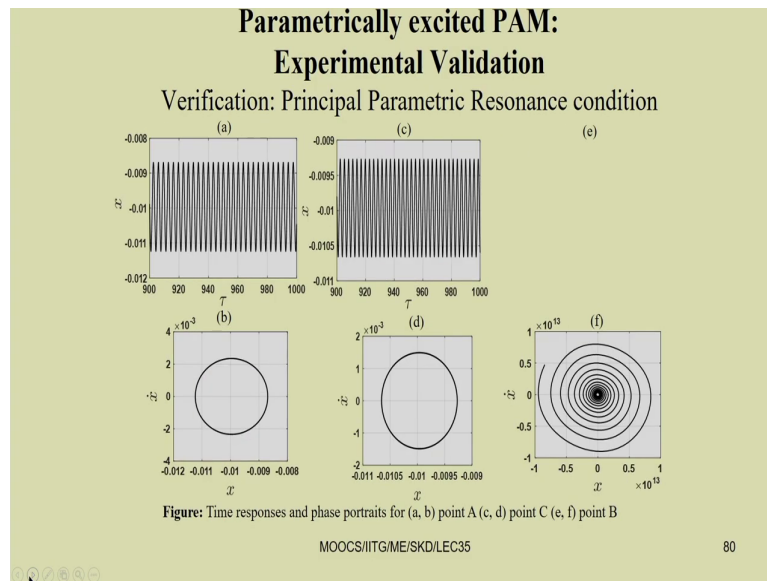


And then from this linear curve fit we can put the linear curve fit and we can get the muscle parameter.

(Refer Slide Time: 64:19) .



(Refer Slide Time: 64:22)



(Refer Slide Time: 64:24)

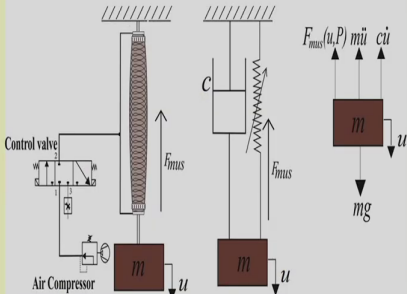
Conclusion: Dynamics of Parametrically Excited PAM

- The higher order MMS is more suitable which provides a conservative results for the system under simple resonance condition.
- For principal parametric resonance condition, it is not required to go for higher order MMS as almost same results can be achieved with the first order MMS.
- The unstable region in the instability plot will decrease with the increase in the value of damping parameter and observed at higher value of the dynamic pressure for both the resonance conditions.
- The variation in the trivial state instability regions is not prominent for the two muscle parameters d_1 and d_2 with both the resonance conditions.
- The highest and lowest values of P_{0cr} are obtained 142.4 kPa and 15 kPa with variation in $c_3 = -0.001 \text{ N/kPa}^2$ and $\mu = 0.001$ respectively for simple resonance condition.
- For principal parametric resonance condition, the highest and lowest values of P_{0cr} are noticed as 142.9 kPa and 2 kPa with variation in $\mu = 0.1$ and $P_m = 200 \text{ kPa}$, respectively.

(Refer Slide Time: 64:25)

System for Case III

Nonlinear Dynamics of Parametrically Excited PAM



- The temporal equation of motion of the system by including the cubic nonlinear term (Ku^3) into the muscle force.

$$\frac{d^2x}{d\tau^2} + 2\epsilon\mu \frac{dx}{d\tau} + x + \epsilon(p_1 \sin \Omega\tau + p_2 \cos 2\Omega\tau)x + \epsilon\alpha x^3 = \epsilon(f_1 + f_2 \sin \Omega\tau)$$

MOOCS/IITG/ME/SKD/LEC35 82

So, taking those muscle parameters, so it has been also verified that the experimental and theoretical values are coming to be similar. So, one can study combined response also. So, previous case we have not taken this nonlinearity.

(Refer Slide Time: 64:42)

Parametrically Excited PAM

- By using the [second order MMS](#), the reduced equations can be written as follows.

- Principal parametric resonance condition, $\Omega \approx 2$

$$a' = \frac{da}{dt} = \varepsilon \left(-\mu a + \frac{p_1 a}{4} \cos 2\gamma \right) + \frac{\varepsilon^2 (1+2\mu)}{2} \left(-\frac{p_1 a}{4} \sin 2\gamma - \frac{3\alpha a^3}{8} \right) + \varepsilon^2 \left[\frac{p_1 p_2 a \cos 2\gamma}{8(1-(3+2\varepsilon\sigma)^2)} \right. \\ \left. - \frac{\alpha p_1 a^3 \cos 2\gamma}{128} + \frac{p_1 p_2 a \cos 2\gamma}{8(1-(3+\varepsilon\sigma)^2)} - \frac{\alpha p_2 a^3 \sin 4\gamma}{128} - \frac{3\alpha p_1 a^3 \cos 2\gamma}{16(1-(3+\varepsilon\sigma)^2)} + \frac{3\alpha p_2 a^3 \sin 4\gamma}{16(1-(3+2\varepsilon\sigma)^2)} \right]$$

$$a\gamma' = a \frac{d\gamma}{dt} = \frac{\alpha\varepsilon\sigma}{2} - \varepsilon \left(\frac{p_1 a}{4} \sin 2\gamma + \frac{3\alpha a^3}{8} \right) - \frac{\varepsilon^2 (1+2\mu)}{2} \left(-\mu a + \frac{p_1 a}{4} \cos 2\gamma \right) - \varepsilon^2 \left[-\frac{p_1^2 a}{8(1-(3+\varepsilon\sigma)^2)} \right. \\ \left. + \frac{p_1 p_2 a \sin 2\gamma}{8(1-(3+2\varepsilon\sigma)^2)} + \frac{\alpha p_1 a^3 \sin 2\gamma}{128} + \frac{p_1 p_2 a \sin 2\gamma}{8(1-(3+\varepsilon\sigma)^2)} - \frac{p_2^2 a}{8(1-(3+2\varepsilon\sigma)^2)} + \frac{\alpha p_2 a^3 \cos 4\gamma}{128} \right. \\ \left. - \frac{p_2^2 a}{8(1-(3+2\varepsilon\sigma)^2)} - \frac{3\alpha p_1 a^3 \sin 2\gamma}{16(1-(3+\varepsilon\sigma)^2)} - \frac{3\alpha p_2 a^3 \cos 4\gamma}{16(1-(3+2\varepsilon\sigma)^2)} + \frac{3\alpha^2 a^5}{256} \right]$$

MOOCS/IITG/ME/SKD/LEC35

83

(Refer Slide Time: 64:43)

Parametrically Excited PAM

- Simultaneous resonance condition, $\Omega \approx 1$

$$a' = \frac{da}{dt} = \varepsilon \left(-\frac{f_2}{2} \cos \gamma - \mu a - \frac{p_2 a}{4} \sin 2\gamma \right) + \frac{\varepsilon^2 (1+2\mu)}{2} \left(\frac{f_2}{2} \sin \gamma - \frac{p_2 a}{4} \cos 2\gamma - \frac{3}{8} \alpha a^3 \right) + \varepsilon^2 \left[\frac{f_1 p_1}{4} \cos \gamma + \frac{\alpha a^3 p_2}{128} \sin 2\gamma + \frac{3 \alpha p_2 a^3}{16(1-(3+2\varepsilon\sigma)^2)} \sin 2\gamma \right]$$

$$a\gamma' = a \frac{d\gamma}{dt} = a\varepsilon\sigma - \varepsilon \left(-\frac{f_2}{2} \sin \gamma + \frac{p_2 a}{4} \cos 2\gamma + \frac{3}{8} \alpha a^3 \right) - \frac{\varepsilon^2 (1+2\mu)}{2} \left(-\frac{f_2}{2} \cos \gamma - \mu a - \frac{p_2 a}{4} \sin 2\gamma \right) - \varepsilon^2 \left[\frac{f_1 p_1}{4} \sin \gamma - \frac{p_1^2 a}{8(1-\varepsilon^2\sigma^2)} + \frac{p_1^2 a}{8(1-(2+\varepsilon\sigma)^2)} - \frac{p_2^2 a}{8(1-(3+2\varepsilon\sigma)^2)} + \frac{\alpha a^3 p_2}{128} \cos 2\gamma - \frac{3 \alpha p_2 a^3 \cos 2\gamma}{16(1-(3+2\varepsilon\sigma)^2)} + \frac{3 \alpha^2 a^5}{256} \right]$$

MOOCS/IITG/ME/SKD/LEC35 84

Here one can take the nonlinearity also by taking the nonlinearity system. Again different resonance conditions can be studied. So, one can study the principle parametric resonance conditions, omega nearly equal to 2. Then simultaneous resonance conditions where omega equal to 1.

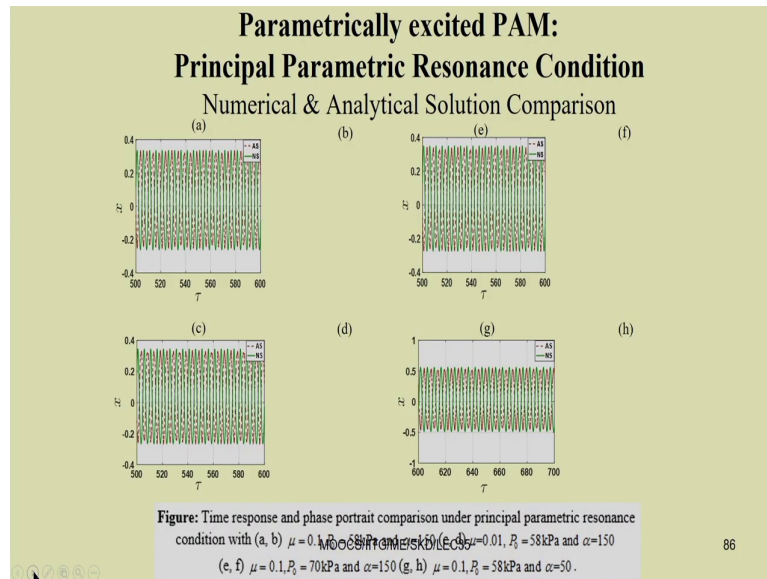
(Refer Slide Time: 64:55)

System Parameter Values for Case III

- The different system parameter values used in the study of numerical simulation.

Parameter	Numerical Value	Parameter	Numerical Value
l_{max}	74 mm	m	6 N
c_1	-234.25 N	ε	0.1
c_2	1.96 N/kPa	α	150
c_3	-0.003 N/kPa ²	p_m	300 kPa
d_1	-100 N	p_0	58 kPa
d_2	1 N/kPa	r	1
μ	0.01		

(Refer Slide Time: 64:56)



(Refer Slide Time: 64:58)

Parametrically excited PAM: Principal Parametric Resonance Condition Trivial State Instability Region

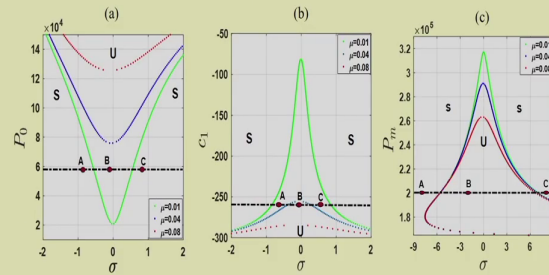
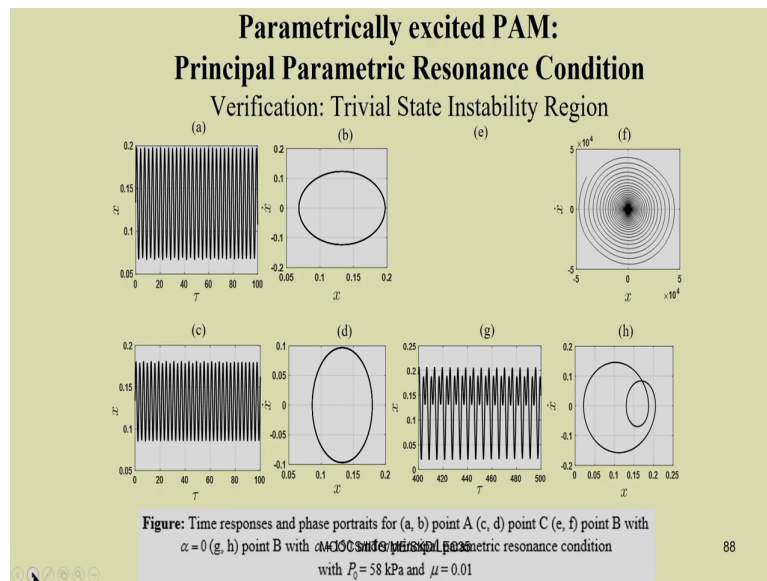
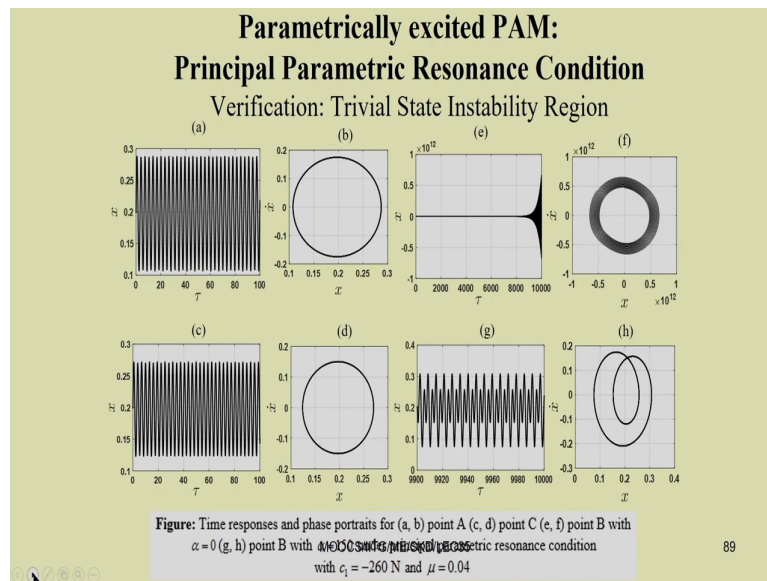


Figure: Trivial state instability region for $\mu = 0.01, 0.04$ and 0.08 under principal parametric resonance condition with (a) $P_0 - \sigma$ (b) $c_1 - \sigma$ (c) $P_n - \sigma$.

(Refer Slide Time: 64:59)

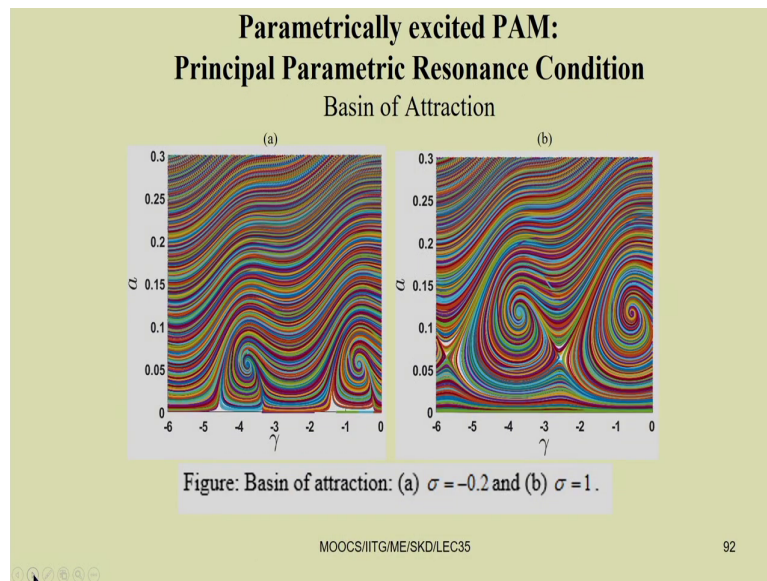


(Refer Slide Time: 65:01)



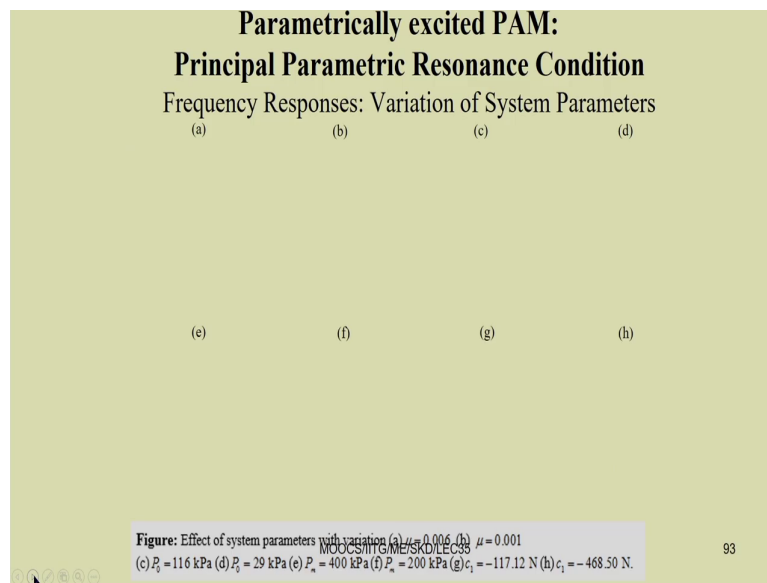
And so these responses can be obtained.

(Refer Slide Time: 65:03)



And, so for different application purpose one can study these responses here clearly one can draw the basin of attraction to study the when there is multiple solutions. So, this basin of attractions can be plotted to get the physical realizations. So, for what initial condition the system will have this response? So, clearly you can see so this is the saddle node point, this is also a saddle node point. So, these are the these are the stable points. So, it is coming to these stable points.

(Refer Slide Time: 65:40)



So, here also you can see this basin of attraction. So, this way so you can study different pneumatic artificial muscle for different application purpose and you may model these as a force excited or direct excited or parametrically excited system.

So, next class we are going to study some other systems, particularly where we will discuss regarding the chaotic response and how to control the chaos in different systems.

Thank you very much.